RESEARCH

Multi-isotopic study of the earliest mediaeval inhabitants of Santiago de Compostela (Galicia, Spain)

Patxi Pérez-Ramallo[1,2,3] · Aurora Grandal-d´Anglade[4] · Elia Organista[5,6] · Elena Santos[7] · David Chivall[8] · Ricardo Rodríguez-Varela[9,10] · Anders Götherström[9,10] · Francisco Etxeberria[3] · Jana Ilgner[1,2] · Ricardo Fernandes[2,11,12] · Juan Luis Arsuaga[13] · Petrus Le Roux[14] · Tom Higham[15] · Julia Beaumont[16] · Hannah Koon[16] · Patrick Roberts[1,2,17]

Abstract

Santiago de Compostela is, together with Rome and Jerusalem, one of the three main pilgrimage and religious centres for Catholicism. The belief that the remains of St James the Great, one of the twelve apostles of Jesus Christ, is buried there has stimulated, since their reported discovery in the 9th century AD, a significant flow of people from across the European continent and beyond. Little is known about the practical experiences of people living within the city during its rise to prominence, however. Here, for the first time, we combine multi-isotope analysis ($\delta^{13}C$, $\delta^{15}N$, $\delta^{18}O_{ap}$, $\delta^{13}C_{ap}$ and $^{87}Sr/^{86}Sr$) and radiocarbon dating (^{14}C) of human remains discovered at the crypt of the Cathedral of Santiago to directly study changes in diet and mobility during the first three centuries of Santiago's emergence as an urban centre (9th–12th centuries AD). Together with assessment of the existing archaeological data, our radiocarbon chronology broadly confirms historical tradition regarding the first occupation of the site. Isotopic analyses reveal that the foundation of the religious site attracted migrants from the wider region of the northwest corner of the Iberian Peninsula, and possibly from further afield. Stable isotope analysis of collagen, together with information on tomb typology and location, indicates that the inhabitants of the city experienced increasing socioeconomic diversity as it became wealthier as the hub of a wide network of pilgrimage. Our research represents the potential of multidisciplinary analyses to reveal insights into the origins and impacts of the emergence of early pilgrimage centres on the diets and status of communities within Christian mediaeval Europe and beyond.

Keywords Paleodiet · Mobility · Camino de Santiago · Pilgrimage · Santiago de Compostela · Middle Ages

Introduction

Pilgrimages to sites of spiritual significance remain one of the most important aspects of organised religion in the 21st century, attracting millions of people each year who often undertake journeys of thousands of kilometres (Collins-Kreiner 2010). The seasonal influx of pilgrims to particular sites can provide a major financial boost to local economies and bolster the political and cultural significance of certain key centres and nations (Collins-Kreiner 2010; Vijayanand 2012; Abuhjeeleh 2019). Pilgrimages can constitute an

essential aspect of certain religions (Collins-Kreiner 2010) or represent an established custom which is not part of core religious tenets (Kim et al. 2016) and have a deep history in various parts of the world. Christian pilgrimage practices begin early, around the 4th century AD, with visits to sites in the Near East associated with the life and martyrdom of Jesus of Nazareth such as the Church of the Holy Sepulchre or the Mount of Olives (Freeman 2011). These continue to be visited today by Christians en mass (Collins-Kreiner and Kliot 2000). Into the early first millennium AD, however, pilgrim sites expanded widely across the Near East and into Europe with objects and body parts associated with Jesus of Nazareth, his disciples and various saints or martyrs acting as attractions for devotees seeking favours and redemption (Freeman 2011).

By the 9th century AD, through the influence of Charlemagne and the expansion of Christianity, much of western

✉ Patxi Pérez-Ramallo
 ramallo@shh.mpg.de

✉ Patrick Roberts
 roberts@shh.mpg.de

Extended author information available on the last page of the article

Europe became firmly gripped by a desire to attain and visit relics and undertake pilgrimages (Freeman 2011). One of the primary centres for pan-European pilgrimages was, together with Rome and Jerusalem, Santiago de Compostela (Galicia, Spain) (Fig. 1). During the first third of the 9th century AD, a purported revelation to a local bishop, Theodomir of Iria, led to the discovery of the sepulchre of the apostle Saint James the Great (López Alsina 2015). In Christian texts, St James was documented as being one of the most prominent apostles of Jesus of Nazareth, martyred by Herod of Agrippa in Jerusalem sometime between 41 and 44 AD (Sulai Capponi 2006). He became an Iberian Christian symbol of the fight against the 'infidel', boosted by different legends reporting battle apparitions during the wars against the Islamic Caliphates (Ramírez Pascual 2004). The supposed discovery of the burial place of Saint James the Great in its Cathedral thus made the city of Santiago de Compostela the destination of thousands Cristian pilgrims. Whilst the site also became an important place of burial, with archaeological investigation revealing a series of different tomb types ranging from the first temple on the site through to the peak of Santiago as a centre of pilgrimage (Guerra Campos 1982), the chronological and architectural development of the Cathedral area has remained relatively unstudied since the mid-20th century (Pérez Ramallo 2021).

Furthermore, although documentary and archaeological sources provide valuable information about the first inhabitants of Santiago de Compostela, as well as the types of foods that were available and how they were probably prepared for consumption, they cannot tell us, with certainty, from where the first inhabitants of the site and later pilgrims came

from, the types of foods they ate and what are the differences existed between the individuals inhumed in the different areas of Santiago de Compostela. Stable isotope analysis of carbon ($\delta^{13}C$) and nitrogen ($\delta^{15}N$) has been regularly used in archaeological contexts to document dietary variation amongst human and animals (Froehle et al. 2012; Makarewicz and Sealy 2015; Webb et al. 2014) and, specifically, there is now a significant literature of stable isotope studies focused on dietary variation across the mediaeval Iberian Peninsula (i.e. Alexander et al. 2015; Jiménez-Brobeil et al. 2016; Mundee 2010; Pérez-Ramallo et al. 2022; Salazar-García et al. 2014). The method is based on the premise that the $\delta^{13}C$ and $\delta^{15}N$ values of human and other animal tissues are directly related to their diet (Ambrose and Norr 1993; Yoder 2012). Meanwhile, combination of stable oxygen isotope ($\delta^{18}O_{ap}$) and strontium isotope analysis ($^{87}Sr/^{86}Sr$) of tooth enamel provides a mean to investigate past human and animal mobility between geologically and hydrologically different regions (Makarewicz and Sealy 2015) and has also been applied in mediaeval Iberian contexts (López-Costas et al. 2021; Pérez Ramallo 2021).

$\delta^{13}C$ variability in terrestrial ecosystems is mainly driven by differential isotopic discrimination against ^{13}C during CO_2 absorption by plants following the two dominant photosynthetic pathways, C_3 (e.g. wheat, barley, trees, shrubs and most temperate grasses) and C_4 (e.g. millet and most tropical grasses) (Smith and Epstein 1971). Whilst bone and dentine collagen $\delta^{13}C$ primarily reflects protein contributions to the diet (Ambrose and Norr 1993; Howland et al. 2003; Jim et al. 2004), tooth enamel $\delta^{13}C$ provides a 'whole diet' signature during the period of enamel formation

Fig. 1 Map of the Iberian Peninsula showing the location of Santiago de Compostela and the other sites mentioned in the text
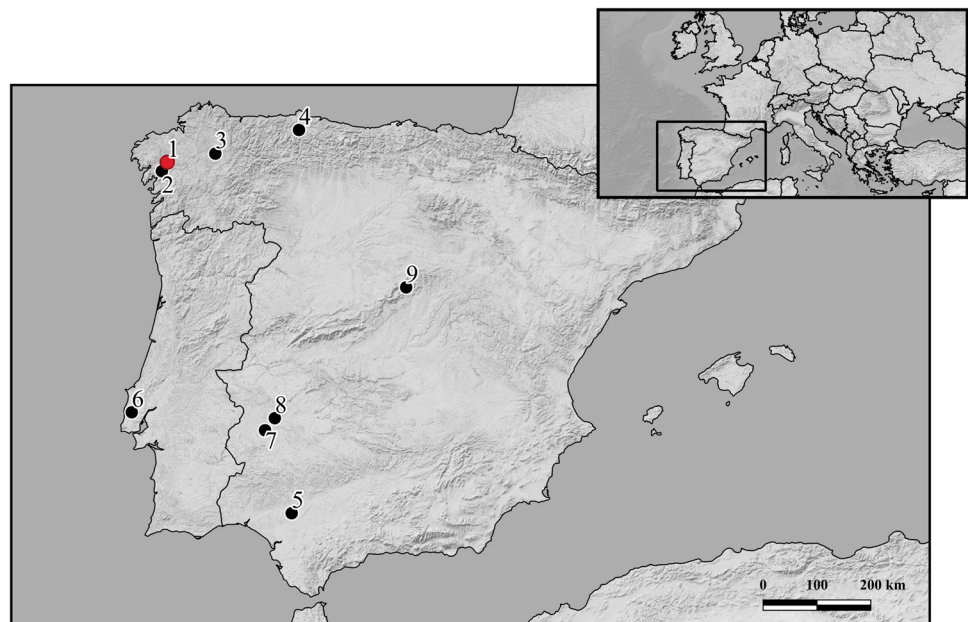
1. Santiago de Compostela; 2. Iria-Flavia, Padrón; 3. Lugo; 4. Oviedo; 5. Seville; 6. Bolores, Portugal; 7. La Pijotilla, Badajoz; 8. Mérida; 9. Madrid

(including carbohydrates, proteins and lipids) (Ambrose and Norr 1993), though the periods of life covered by each tissue will vary depending on the exact element sampled (Gregoricka et al. 2017). $\delta^{15}N$ varies with trophic level, with changes of $+2$ to $+6‰$ between plants and herbivores and herbivores and their consumers being well-documented in both aquatic and terrestrial systems (Tieszen and Fagre 1993; DeNiro and Epstein 1981; Sealy et al. 1987). The long length of marine food chains leads to distinctively high $\delta^{15}N$ in marine foods and consumers compared to their terrestrial counterparts. Marine resources also have higher $\delta^{13}C$ values than terrestrial C_3 ecosystems that mimic those of C_4 plants, due to a different source of CO_2 for primary producers (Schoeninger and DeNiro 1984). Freshwater organisms also tend to have high $\delta^{15}N$, though their $\delta^{13}C$ is highly variable (Dufour et al. 1999). Whilst these distinctions provide a firm basis for palaeodietary exploration, it is important to note that external environmental conditions such as temperature, aridity, rainfall or crop growing conditions (e.g. the application of manure) can also influence the $\delta^{13}C$ and $\delta^{15}N$ values (Amundson et al. 2003; Bogaard et al. 2007). Thus, the analysis of associated animals or plants remains important (Casey and Post 2011).

$\delta^{18}O_{ap}$ is directly related to that of drinking water, which, in turn, is known to vary predictably geographically (Longinelli 1984; Lécolle 1985). This variation is driven by changes in the $\delta^{18}O$ of precipitation and groundwater (Makarewicz and Sealy 2015; Webb and White 2014). Equations such as those presented by Longinelli (1984) or Levinson et al. (1987) are often used to convert tooth enamel carbonate or phosphate $\delta^{18}O$ into a drinking water $\delta^{18}O$, yet significant errors and uncertainties are associated (Lightfoot and O'Connell 2016). Furthermore, changes in climate through time can affect local drinking water $\delta^{18}O$. As a result, when interpreting whether past human $\delta^{18}O$ correlates to that of 'local' values, it is better to compare them to a local baseline of associated animal $\delta^{18}O$. Even then, intra-population variability is known to be significant (Lightfoot and O'Connell 2016). Strontium isotope ($^{87}Sr/^{86}Sr$) approaches to past human mobility rest on the premise that rocks of different ages and lithologies have different $^{87}Sr/^{86}Sr$ values, which do not alter as strontium is passed from the source rocks into the biosphere without isotopic fractionation (Evans et al., 2006). Although there is no mass-dependent fractionation from the bedrock into a given food chain, bedrock $^{87}Sr/^{86}Sr$ does not always correlate directly with bioavailable $^{87}Sr/^{86}Sr$. Differential weathering of rocks with different $^{87}Sr/^{86}Sr$ ratios, as well as the geographic variability of hydrology and aeolian transport, leads to variations in the $^{87}Sr/^{86}Sr$ of soils and plants overlying a given distribution of rocks (Graustein 1989). From plants, Sr^{2+} actively replaces Ca^{2+} in consumer tissues as part of the process of nutrient uptake and excretion (Graustein 1989), with the amount of strontium incorporated into the skeleton believed to be directly reflective of that available from the local environment (Montgomery 2010). A robust bioavailable baseline is essential as the $^{87}Sr/^{86}Sr$ of an individual will be the combined consequence of all food consumed and all water imbibed, as well as the extent of the range over which an individual obtains food and drink (Montgomery 2010).

A multi-isotope approach has huge potential to provide direct insights into the origins and diets of individuals living at Santiago de Compostela during its foundation and expansion as a major mediaeval religious centre. Nevertheless, to date, there has been no extensive bioarchaeological and chronological study of the origin and development of the Cathedral and its necropolis at the heart of this Christian centre during the late first and early second millennium AD. Here, we aim to investigate the lifeways, status and origin of its first inhabitants during the birth and formation of Santiago de Compostela using $\delta^{13}C$ and $\delta^{15}N$ analysis of bone and dentine collagen and $\delta^{18}O_{ap}$, $\delta^{13}C_{ap}$ and $^{87}Sr/^{86}Sr$ analysis of tooth enamel. Alongside new chronological information obtained using ^{14}C analysis of some of the same human remains, we examine the dietary and mobility patterns of the first mediaeval inhabitants and pilgrims of Santiago de Compostela and contrast the obtained results with the available historical sources and previous archaeological research to explore the wider economic, dietary and geographical situation of these populations.

Archaeological, historical and geographical background

After the discovery of the tomb of St James by the bishop Teodomirs, Alfonso II, King of Asturias, became the first pilgrim to visit Santiago de Compostela in 814 AD, establishing the first pilgrimage route, known as *El Camino Primitivo* (The Primitive Way) (López Alsina 2015), linking his capital in Oviedo to Santiago de Compostela. Between the 11th and 14th centuries AD, Santiago de Compostela received hundreds of thousands of pilgrims (Martínez García 2004; Gerrard and Gutiérrez-González 2018) arriving from across the continent via various *Caminos de Santiago*, pilgrimage routes that eventually sprawled across Spain, Portugal, France, Germany and other parts of Europe. The new, growing political and cultural status of Santiago de Compostela saw its local population expand, likely attracting people from around the region through its novel socioeconomic opportunities. The Black Death and the division of the Christian churches resulted in a decline in the number of pilgrims in the 15th century and numbers remained limited through to the 20th century (Miranda García 2002). Today, the city and its Caminos are UNESCO World Heritage sites, and 300,000 pilgrims visit Santiago de Compostela every

year on spiritual journeys popularised in literature and film (Millán Vásquez de la Torre et al. 2010; González 2018; Álvarez-Sousa 2015).

Nowadays, Santiago de Compostela is the capital of the region of Galicia (Spain) in the northwest of the Iberian Peninsula (Fig. 1). The site has, following the Köppen classification, a temperate oceanic climate (Cfb), with mild to warm and moderately dry summers and mild, wet winters (Agencia Estatal de Metereología). A combination of winds from the Atlantic and the surrounding mountains provides Santiago de Compostela with one of the highest rainfalls in Spain at 1787 mm per year (Agencia Estatal de Metereología). Geologically, there are two parts of the city. The North and East of the city lie above a *Complejo de Órdenes* (the Ordes Complex), formed by metamorphosed ultrabasic rocks. By contrast, the west sits above granite intrusions, composed mainly of leucogranites of two micas and migmatites granitoid (Martínez Catalán et al. 1984). The Order Complex consists mainly of metasediments, along with some materials that come from the oceanic rock bottom itself, and some with volcanic origin: orthogenesis, amphibolite and gabbro intrusions (Martínez Catalán et al. 1984). These sedimentary materials derive mainly from Final Precambrian and Lower Palaeozoic materials, and their regional metamorphism occurred during the Hercynian orogeny in the Upper Palaeozoic (Fig. 2).

Based on previous archaeological work, three different phases of occupation have been distinguished for Santiago de Compostela: High Middle Ages (9th-12th centuries AD), Germanic or Early Middle Ages (5th-7th centuries AD) and Roman Ages (1st-5th centuries century AD) (Chamoso Lamas 1957; López Alsina 2015; Guerra Campos 1982). Between at least the 8th century AD, until the discovery of the apostolic tomb, the place was uninhabited, with small rural populations in its surroundings (López Alsina 2015). These phases of occupation at Santiago de Compostela were established via the archaeological excavations conducted under the current Cathedral of Santiago de Compostela at the end of the 19th century and between 1946 and 1959 (Chamoso Lamas 1957; Guerra Campos 1982). During the latter archaeological works of the mid-20th century, the remains of the two previous temples, the first city wall and a mediaeval necropolis with a Roman origin were identified (Guerra Campos 1982) (Fig. 3 and S1). This mediaeval necropolis (9th-12th centuries AD) corresponds to the cemetery that surrounded the temple created by order of Alfonso II after the discovery of St James's tomb (820/830–872 AD) (Chamoso Lamas 1957; López Alsina 2015; Guerra Campos 1982) and the one raised 40 years later over the first church, the basilica of Alfonso III (872–1075 AD) (López Alsina 2015). During these three centuries, the mediaeval necropolis spread significantly, resulting in an overlap of tombs caused by the temple's delimited location on top of

a hill (Fig. S1). During the archaeological excavations conducted in mid-20th century, attempting to find the oldest part of the necropolis, the archaeologists destroyed a significant number of tombs (Guerra Campos 1982). Fortunately, the remaining graves and their individuals (n = 33) were respected without alterations. From those, 5 individuals (4 adults and 1 juvenile) were partly analysed via osteological techniques in 1972 and 1982 (Pedreira Barros 1972; Carro Otero and Varela Ogando 1982). Since then, the necropolis of the Cathedral of Santiago de Compostela had lacked any new archaeological work, including the application of multidisciplinary approaches, with the exception of interpretive revisions of the existing data by Chamoso Lamas (e.g. Suárez Otero 2015).

In 2015, a pilot osteological study, combined with stable carbon (δ^{13}C), nitrogen (δ^{15}N) and oxygen (δ^{18}O) isotope analysis, was carried out on eight individuals excavated in situ from the mediaeval necropolis of the Cathedral of Santiago de Compostela and analysed at the Stable Isotope Laboratory, University of Bradford (Bradford, the UK) (Pérez Ramallo 2015), along with a small sample of contemporaneous faunal remains. The measurement of human enamel carbonate demonstrated that 6 of the 8 individuals had childhood δ^{18}O values suggesting a non-local origin (Müldner et al. 2009)—for a summary of the method, see Britton (2020). In addition, incremental dentine collagen δ^{13}C and δ^{15}N produced using Beaumont et al. (2013) method, and with age assigned using Beaumont and Montgomery (2015), demonstrated changes in the diet of these individuals through the years of tooth formation and to rib bone collagen δ^{13}C and δ^{15}N in adulthood (Tab. S1). These data showed significant variations probably because of geographic mobility (NCS003) (Fig. S2; Tab. S1) and/or change of social status, as well as potential short-term dietary patterns consistent with C_4 consumption during periods of famine (NCS006 and NCS007) (Fig. S2; Tab. S1). Nevertheless, the sample size remained too small for definitive conclusions, and the chronology of the burials required confirmation.

The site of Santiago de Compostela and the human remains found in it

Following the pilot work in 2015, we sought to continue the investigation of the remaining individuals buried in situ at the mediaeval Necropolis of Santiago de Compostela, with the objective to better understand the lifeways, status and origin of its first inhabitants during the origins and formation of Santiago de Compostela as a religious hub. In 2017, we conducted new fieldwork examining the remains of individuals recovered during the mid-20th century (Fig. 3 and S1), increasing the number of individuals analysed and analytical methods applied. We divided the necropolis into 3 zones in

Fig. 2 Map illustrating the different geological areas based on bedrock, following Instituto Geológico y Minero de España, Magna 1:50.000 (2ª Serie), Hoja 94 (https://mapas.igme.es/gis/rest/services/Cartografia_Geologica/IGME_MAGNA_50/MapServer). A, Santiago de Compostela. B, Rochaforte Castle. 1, Metabasic rocks; 2, Órdenes schists; 3, Schists and paragneiss; 4, Biotite orthogneises; 5, Shales with quartzite levels; 6, Granite of two micas; 7, Migmatitic granitoid
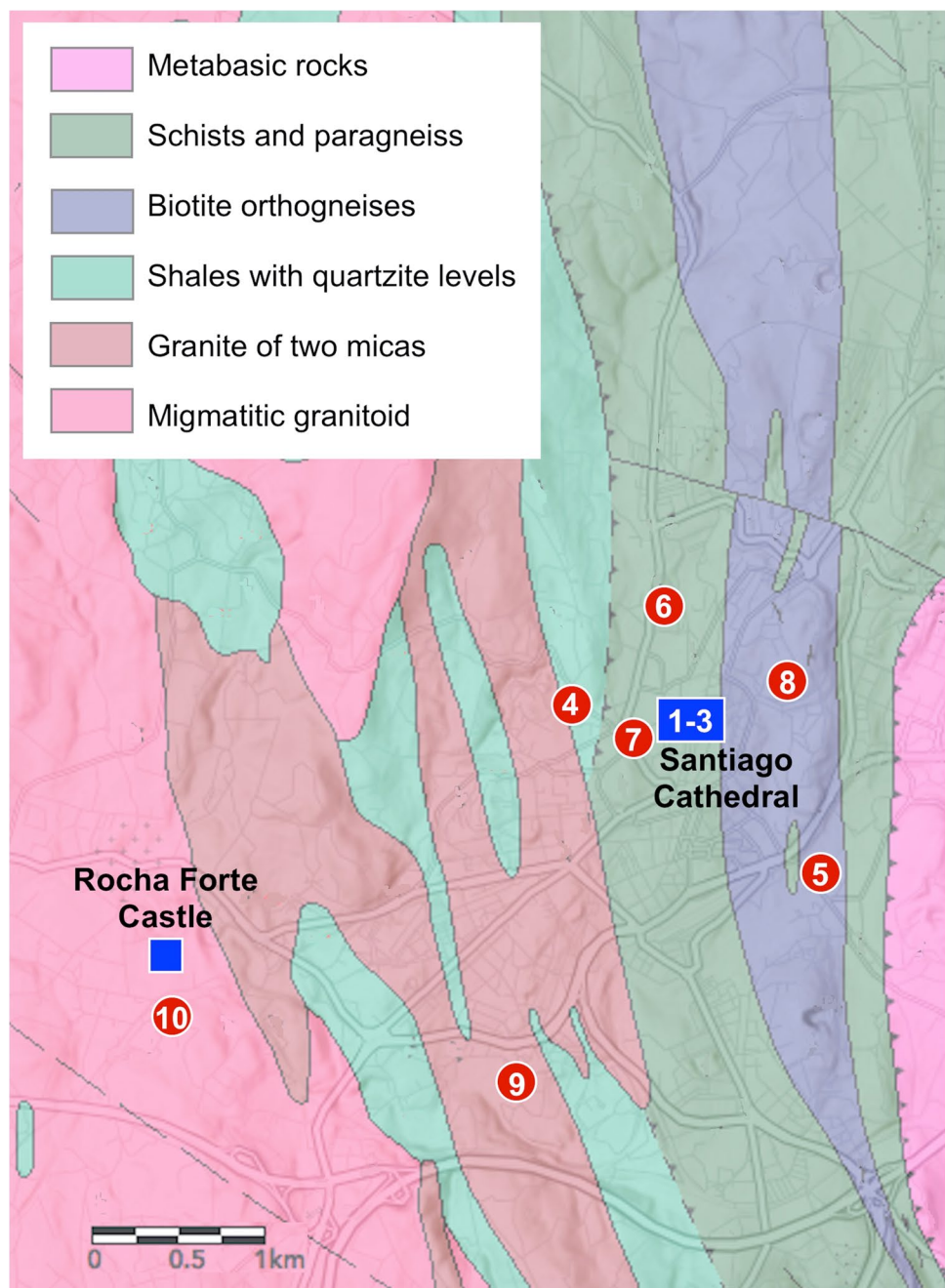
relation to their position relative to the Basilica of Alfonso III (Fig. 3). The first two zones (1 and 2) correspond to privileged areas around the entrances to the basilica, which were the locations closest to the relics, and in the case of zone 2 where different elite personages and bishops were buried (e.g. Teodomirs) (Guerra Campos 1982). Meanwhile, zone 0 is the broadest, most intensely occupied and most distant from Alfonso III's temple (Fig. 3 and S1).

Osteological analysis is a non-destructive technique that is focused on human skeleton recovery and interpretation. We performed macroscopic observations using the naked eye and a magnifying lens. Sex assessment and age estimations of the skeletons were made using established morphological criteria of the skull, pelvis, tooth wear and long bones following Buikstra and Ubelaker (1994); Brooks and Suchey (1990); Brothwell (1981); Klales et al. (2012); Mays (2010); Meindl and Lovejoy (1985); Lovejoy et al. (1985); Walker (2008) and Bass (2005). However, the amount of bone elements recovered, the local substrate that accelerated their degradation (López-Costas and Müldner 2016; Kaal et al. 2016), limited the osteological analysis. We were able to estimate the sex for a total of 9 female, 11 male and
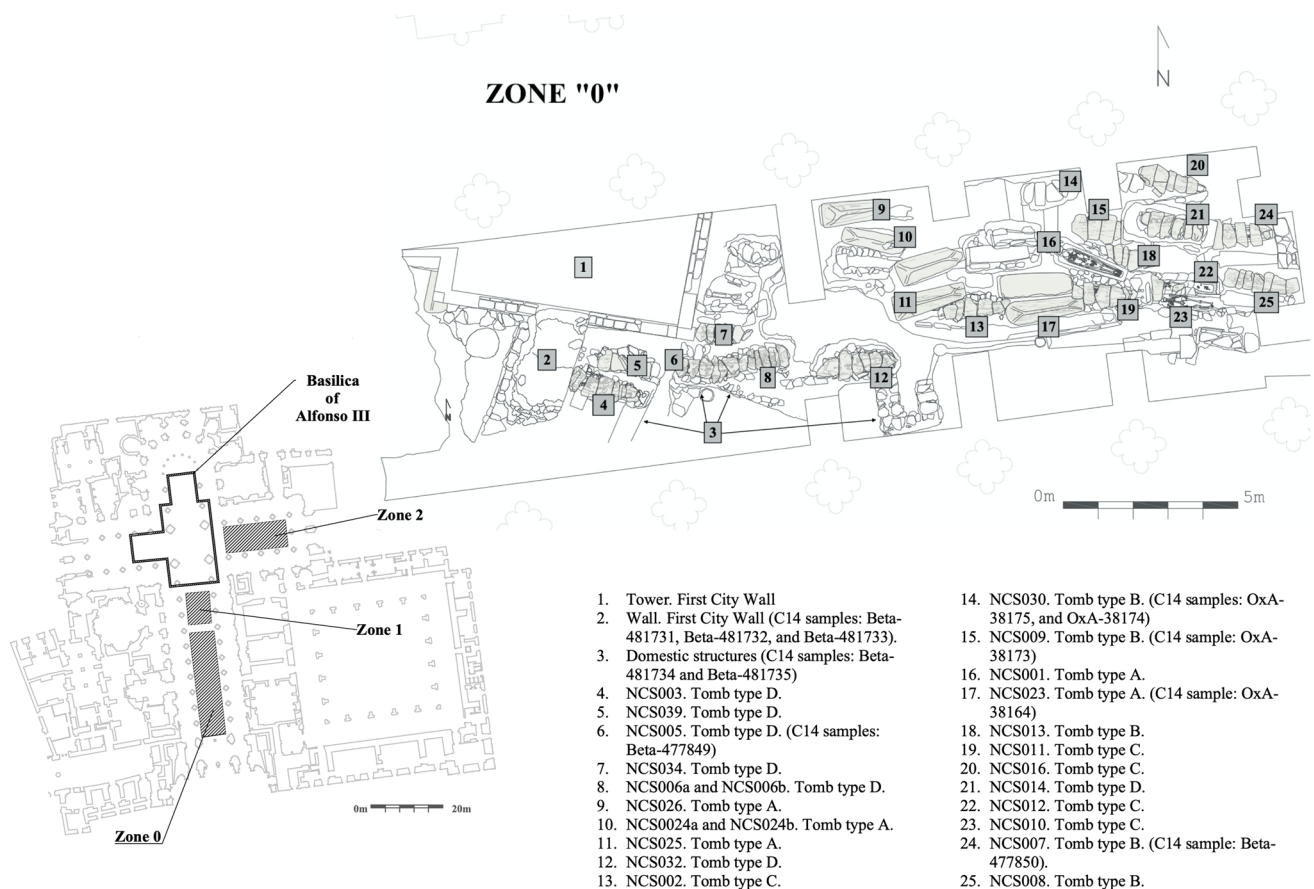
Fig. 3 Zoomed in map of the main and better conserved area of the mediaeval necropolis, zone "0", and a zoomed-out map of the Cathedral of Santiago de Compostela indicating the location of the Basilica of Alfonso III (872–1075), and the position of all three zones of the mediaeval necropolis

13 indeterminate. These were divided into groups of age following the criteria of Buikstra and Ubelaker (1994) as follows: 2 children, 7 young adults, 7 middle adults and 4 old adults. The remaining individuals (n = 14) were classified here as indeterminate adults (Table 1).

To establish the chronology of the buried individuals, and the phases of occupation, we employed radiocarbon dating. We radiocarbon-dated 9 human bone samples in order to confirm the chronology and understand the development of the necropolis over time alongside the Cathedral complex (Fig. 4; Tab. S2). Of these, 7 samples were analysed at the Oxford Radiocarbon Accelerator Unit (ORAU), Oxford, UK. These represented human bone from the tomb types 'Sarcophagus' (stone sarcophagus), 'Cists' and 'Anthropomorphic' (rectangular, oval or anthropomorphic tombs excavated into the geological substrate with stone walls or rectangular slabs, covered with thick or thin slabs, respectively), distributed amongst the three areas of the necropolis (Figs. 3, 5, and S1). Meanwhile, 2 samples of bone from zone '0', from tombs type 'Cists' and 'Rectangular' (rectangular tomb with irregular stone walls and cover, with a soil base), were

sent to Beta Analytic Inc. Radiocarbon Laboratory, Florida, USA. The full protocol and standards used in each laboratory are reported in the supplementary information text S1. Radiocarbon determinations were calibrated using OxCal v4.4 and the IntCal20 calibration curve (Reimer et al. 2020).

The radiocarbon dating results suggest that the individuals analysed in this study date to between the 9th and 12th centuries AD (Fig. 4; Tab. S2) and have confirmed that the different tomb types identified during the first excavations during the mid-20th century excavations (Guerra Campos, 1982) represent a chronological sequence of necropolis use. Based on our dates, and existing contextual knowledge, the so-called *Doble Estola* sarcophagus (Guerra Campos, 1982), here classified as tomb type 'Sarcophagus' (Figs. 4, 5, and S1; Tab. S2), appears to represent individuals buried during the first decades after the discovery of St James' remains in the 9th century AD. Although a significant number of these tombs were reused, with remains of more than one individual being discovered in some cases within (NCS001, NCS023, NCS024, NCS145 and NCS258), they may even be related to the first temple raised on the site by Alfonso

Table 1 $\delta^{13}C$, $\delta^{15}N$, $\delta^{18}O_{ap}$, $\delta^{13}C_{ap}$, $\delta^{18}O_{dw}$ and $^{87}Sr/^{86}Sr$ data, sex, age and chronology of human from the Necropolis of the Cathedral of Santiago. * = Here we classified these tombs in four categories: Sarcophagus = granite sarcophagi; Cists = tombs with small stones wall or cists, and rectangular or oval-shaped covered with slabs; Anthropomorphic = anthropomorphic tombs excavated in the rock and covered with slabs and Rectangulars = those that have a rectangular shape and made with irregular size stones

Individual reference and zone	Tomb typology and chronology*	Sex and age estimation	Radiocarbon years before present (BP)	Calibrated calendar date (95.4%)	Tooth $\delta^{15}N$ and $\delta^{13}C$ (‰)	Bone $\delta^{15}N$ and $\delta^{13}C$ (‰)	Tooth enamel $\delta^{18}O_{ap}$ and $\delta^{13}C_{ap}$ (‰)	Tooth enamel $\delta^{18}O_{dw}$	Tooth Enamel $^{87}Sr/^{86}Sr$ ± 2 s internal
NCS001 Zone "0"	Sarcophagus 9th–10th centuries AD	Male Middle adult	-	-	-	Rib 8.7 −19.8	-	-	RI¹/11 0.710287±12
NCS002 Zone "0"	Cists 10th–11th centuries AD	Male Middle adult	-	-	LM₂/37 12.2 −16.9	Rib 11.7 −17.3	LM₂/37 −5.4 −10.5	LM₂/37 −8.4	LM₂/37 0.714043±13
NCS003 Zone "0"	Rectangular 11th–12th centuries AD	Female Old adult	-	-	LM₂/37 12.7 −15.8	Rib 12.1 −17.6	LM₂/37 −4.4 −12.1	LM₂/37 −6.7	-
NCS005 Zone "0"	Rectangular 11th–12th centuries AD	Female Young adult	940±30	1028–1172 cal AD	LM₂/37 10.6 −17.8	Rib 10.9 −17.8	LM₂/37 −3.6 −9.0	LM₂/37 −5.4	LM₂/37 0.712123±11 LC¹/23 0.712119±13
NCS006a Zone "0"	Rectangular 11th–12th century AD	Female (?) Indeterminate adult	-	-	-	Rib 10.5 −17.8	-	-	LC₁/33 0.712953±13
NCS006b Zone "0"	Rectangular 11th–12th centuries AD	Female Middle adult	-	-	-	Rib 10.6 −17.4	-	-	RM¹/16 0.712623±12
NCS007 Zone "0"	Anthropomorphic 11th century AD	Male Middle adult	980±30	995–1158 cal AD	LM²/27 10.6 −16.3	Rib 10.9 −18.2	LM²/27 −4.2 −7.5	LM²/27 −6.3	LM²/27 0.712975±13 LM¹/26 0.712688±13
NCS008 Zone "0"	Anthropomorphic 11th century AD	Male Old adult	-	-	-	Rib 11.6 −18.2	-	-	-
NCS009 Zone "0"	Anthropomorphic 11th century AD	Male Middle adult	1014±26	990–1150 cal AD	LM₂/37 10.4 −16.3	Rib 10.8 −17.9	LM₂/37 −4.1 −6.9	LM₂/37 −6.2	LM₂/37 0.710995±12 RM₃/48 0.711278±11
NCS010 Zone "0"	Cists 10th–11th centuries AD	Female Middle adult	-	-	RM²/17 10.6 −15.9	Rib 10.3 −17.5	RM²/17 −4.2 −11.2	RM²/17 −6.3	RM²/17 0.713611±14
NCS011 Zone "0"	Anthropomorphic 10th–11th centuries AD	Male Middle adult	-	-	-	Rib 11.1 −18.0	-	-	RI₁/21 0.714523±13

Table 1 (continued)

Individual reference and zone	Tomb typology and chronology*	Sex and age estimation	Radiocarbon years before present (BP)	Calibrated calendar date (95.4%)	Tooth $\delta^{15}N$ and $\delta^{13}C$ (‰)	Bone $\delta^{15}N$ and $\delta^{13}C$ (‰)	Tooth enamel $\delta^{18}O_{ap}$ and $\delta^{13}C_{ap}$ (‰)	Tooth enamel $\delta^{18}O_{dw}$	Tooth Enamel $^{87}Sr/^{86}Sr$ ± 2 s internal
NCS012 Zone "0"	Anthropomorphic 10th-11th centuries AD	Indeterminate Indeterminate adult	-	-	-	Rib 10.3 −17.0	-	-	-
NCS014 Zone "0"	Rectangular 11th-12th centuries AD	Female Young adult	-	-	-	Rib 11.5 −18.4	-	-	LM²/27 0.709236±15
NCS016 Zone "0"	Cists 11th century AD	Female (?) Young adult	-	-	LM₂/37 11.0 −17.5	Rib 10.8 −17.8	LM₂/37 −2.1 −9.4	LM₂/37 −3.0	LM₂/37 0.713785±13
NCS022 Zone "0"	Sarcophagus 9th-10th centuries AD	Indeterminate Indeterminate adult	-	-	-	-	RM²/17 −3.4 −8.4	RM²/17 −5.0	RM²/17 0.713249±11
NCS023 Zone "0"	Sarcophagus 9th-10th centuries AD	Female Young Adult	1195±26	710–943 cal AD	RM₂/47 10.3 −18.4	-	RM₂/47 −2.9 −12.8	RM₂/47 −4.3	RM₂/47 0.711921±11
NCS024a Zone "0"	Sarcophagus 9th-10th centuries AD	Indeterminate Indeterminate adult	-	-	-	-	-	-	LC¹/23 0.715053±14
NCS024b Zone "0"	Sarcophagus 9th-10th centuries AD	Indeterminate Indeterminate adult	-	-	-	-	Premolar −4.0 −11.5	Premolar −6.0	Premolar 0.711284±15
NCS025 Zone "0"	Sarcophagus 9th-10th centuries AD	Male Indeterminate adult	-	-	LM₂/37 10.3 −20.0	-	LM₂/37 −4.5 −13.0 LM₃/38 −6.2 −13.7	LM₂/37 −6.8 LM₃/38 −9.7	LM₂/37 0.716632±13 LM₃/38 0.716363±13
NCS026 Zone "0"	Sarcophagus 9th-10th centuries AD	Male Young Adult	-	-	-	-	-	-	LM¹/26 0.715172±14
NCS030 Zone "0"	Cists 10th-11th centuries AD	Female Old Adult	1036±27	899–1040 cal AD	-	Metatarsal 10.0 −17.8	-	-	-
NCS032 Zone "0"	Rectangular 11th-12th centuries AD	Indeterminate Indeterminate adult	-	-	LP²/25 11.1 −16.9	Rib 10.3 −17.7	LP²/25 −6.5 −9.2	LP²/25 −10.2	LP²/25 0.713525±13
NCS033 Zone "0"	Rectangular 11th-12th centuries AD	Male Young Adult	-	-	-	Rib 10.9 −16.0	-	-	LP¹/24 0.715638±14

Table 1 (continued)

Individual reference and zone	Tomb typology and chronology*	Sex and age estimation	Radiocarbon years before present (BP)	Calibrated calendar date (95.4%)	Tooth $\delta^{15}N$ and $\delta^{13}C$ (‰)	Bone $\delta^{15}N$ and $\delta^{13}C$ (‰)	Tooth enamel $\delta^{18}O_{ap}$ and $\delta^{13}C_{ap}$ (‰)	Tooth enamel $\delta^{18}O_{dw}$	Tooth Enamel $^{87}Sr/^{86}Sr$ ± 2 s internal
NCS034 Zone "0"	Rectangular 11th-12th centuries AD	Indeterminate Sub-adult (child)	-	-	-	-	-	-	$dlm_2/75$ 0.712822±14
NCS039 Zone "0"	Rectangular 11th-12th centuries AD	Female Old Adult	-	-	$RM^2/17$ 12.0 −15.5	Rib 10.7 −16.6	$RM^2/17$ −3.0 −6.4	$RM^2/17$ −4.4	$RP^1/15$ 0.713102±11 $RM^2/17$ 0.712937±13
NCS145a Zone "1"	Sarcophagus 9th-10th centuries AD	Indeterminate Indeterminate adult	-	-		-	$LM_2/37$ −4.2 −14.2	$LM_2/37$ −6.3	$LM_1/36$ 0.713797±14 $LM_2/37$ 0.711426±10
NCS145b Zone "1"	Sarcophagus 9th-10th centuries AD	Indeterminate Indeterminate adult	-	-		-	$LM_3/38$ −3.4 −10.8	$LM_3/38$ −5.1	$LM_3/38$ 0.715810±14
NCS153 Zone "1"	Cists 10th century AD	Indeterminate Sub-adult (child)	-	-	-	-	-	-	$dm_2/84$ 0.712397±12.8
NCS154 Zone "1"	Cists 10th century AD	Male Indeterminate adult	1119±24	886–992 cal AD	$RP^2/15$ 12.3 −17.6		$RP^2/15$ −3.0 −11.3	$RP^2/15$ −4.4	$RC^1/13$ 0.712863±16 $RP^2/15$ 0.712755±13
NCS256 Zone "2"	Anthropomorphic 11th century AD	Indeterminate Indeterminate adult	-	-	-	Parietal, skull 11.6 −17.2	-	-	-
NCS258a Zone "2"	Anthropomorphic 11th century AD	Indeterminate Indeterminate adult	-	-	-	Parietal, skull 11.9 −18.4	-	-	-
NCS258b Zone "2"	Anthropomorphic 11th century AD	Indeterminate Indeterminate adult	1008±25	991–1150 cal AD	$RM_2/47$ 12.2 −17.8		$RM_2/47$ −4.7 −8.7	$RM_2/47$ −7.3	$RM_2/47$ 0.713665±13 $RM_3/48$ 0.712886±9
NCS259 Zone "2"	Anthropomorphic 11th century AD	Indeterminate Indeterminate adult	-	-	-	Temporal, skull 11.4 −17.2	-	-	-

Fig. 4 Radiocarbon determinations calibrated using OxCal. v4.4 (Bronk Ramsey, 2021) and the IntCal20 atmospheric curve (Reimer et al. 2020)
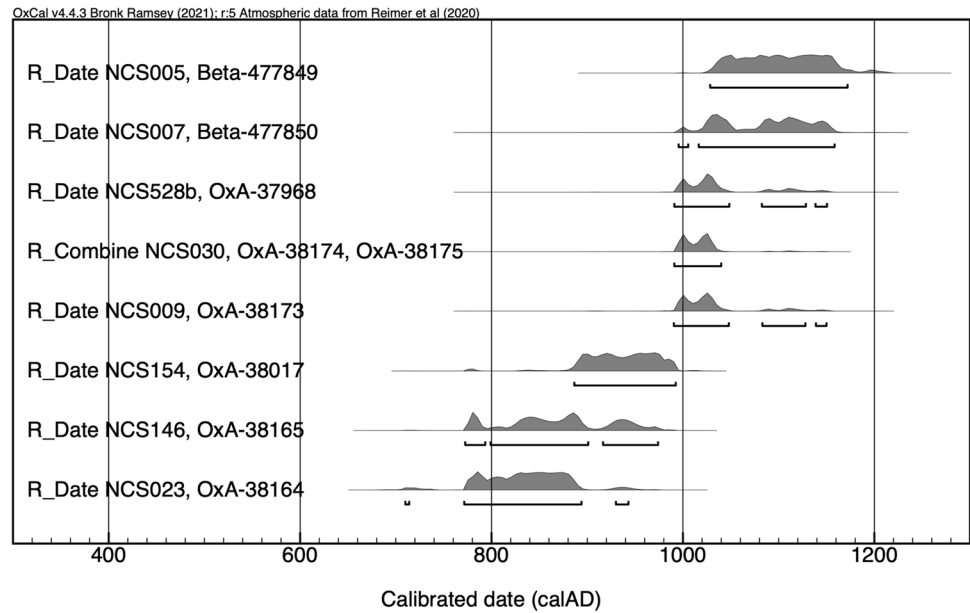

Fig. 5 Tombs typology at the mediaeval necropolis of Santiago de Compostela. **A** Sarcophagus (granite sarcophagi); **B** cists (tombs with small stones wall or cists, and rectangular or oval-shaped covered with slabs); **C** anthropomorphic (anthropomorphic tombs excavated in the rock and covered with slabs); and **D** rectangulars (those that have a rectangular shape and made with irregular size stones)

II (820/830–872). However, their original position changed following the creation of a second shrine constructed during the reign of Alfonso III (872–1075), as it was suggested by Chamoso Lamas (1957), or after the attack of the city in 997 by the Caliphate of Córdoba led by Almanzor (López Alsina 2015; Guerra Campos 1982; Pérez de Tudela y Velasco 1998). After tomb type 'Sarcophagus', the ¹⁴C results and archaeological context show that tomb type 'Cists' appears from at least the 10th century AD, coexisting with tomb type 'Anthropomorphic' during the first half of the 11th century AD (Figs. 4, 5, and S1; Tab. S2). Type 'Rectangular' tombs

date to the latest period of necropolis use (11th–12th centuries AD) (Figs. 4 and 5, and S1; Tab.S2). Tombs of this type had a rectangular shape and were made from irregular-sized stones and a base of soil and rubble, lying over and between the remains of the first city wall and some early domestic structure, and may be connected to an asylum that was built between the ninth and the 10th centuries AD (López Alsina 2015).

The obtained radiocarbon determinations confirm a chronology spanning the development of the mediaeval necropolis of Santiago de Compostela across three broad stages, from the

temple of Alfonso II (820/830–872), through the shrine of Alfonso III (872–1075), up to the development of the Romanesque Cathedral (1075–1211). The direct or indirect consumption of marine proteins by humans could impact ^{14}C quantification, leading to offsets between measured radiocarbon ages from true chronological ages as a consequence of the marine reservoir effect (Fernandes et al. 2016). We face challenges in estimating the exact influence of marine protein on an individual's diet and, therefore, the reliability of radiocarbon estimations using Bayesian modelling. Nevertheless, the radiocarbon dating results fit with the relative chronology expected based on archaeological and historical discussion, despite the fact that many tombs may have been reused (NCS001, NCS005, NCS006, NCS023, NCS024, NCS145 and NCS258). Furthermore, except for individuals NCS154 (δ^{15}N 12.3‰ and δ^{13}C -17.6‰), and NCS258b (δ^{15}N 12.2‰ and δ^{13}C -17.8‰), there is limited obvious evidence for marine resource consumption in the diets of individuals selected for radiocarbon dating (Table 1 and S2). Our results show a more intense and complex use of space than was previously determined by archaeological investigations in the mid-20th century (Guerra Campos 1982).

Materials and methods

To reconstruct the diet and mobility for 33 individuals located in situ at the mediaeval necropolis (9th–12th century AD), we employed carbon (δ^{13}C), nitrogen (δ^{15}N), oxygen (δ^{18}O) and strontium (^{87}Sr/^{86}Sr) isotope analyses. To support the interpretation of these results, we compared them with isotopic analyses performed on faunal samples from the necropolis of Santiago (n = 12) and 32 faunal samples from the nearest Rocha Forte Castle (13th to 15th centuries AD, Santiago de Compostela). The results provide noteworthy insights into the resource access and cultural behaviours.

Materials

To provide insights into the diets, social status and origins of individuals buried in the Santiago Cathedral necropolis, we undertook multi-isotopic analysis (^{87}Sr/^{86}Sr, δ^{18}O, δ^{13}C, δ^{15}N) of 33 human and 41 fauna. From the 33 individuals, we selected 2 osteological samples per individual for δ^{15}N and δ^{13}C analyses. Following the rejection of samples that failed to meet collagen quality requirements (C:N atomic ratios, % collagen), we were left with a total of 34 samples from 25 individuals (Table S3). Due to the relative lack of faunal samples from the necropolis of Santiago (n = 9), we expanded our faunal baseline by adding 32 new individuals from Rocha Forte Castle (13th to 15th centuries AD, Santiago de Compostela) that is thought to represent the

provisions available to the city as a whole during this later period (López-Costas and Teira Brión 2014). Furthermore, to better determine a robust bioavailable ^{87}Sr/^{86}Sr baseline for the city, in addition to faunal teeth from Rocha Forte Castle (n = 15), we analysed ten shells of modern (n = 7) and archaeological (n = 3) snails (Table 2) as they are considered one of the most appropriate materials for integrating local bioavailable strontium (Maurer et al. 2012; Bartelink and Chesson 2019). These were selected from diverse points of the city based on geological substrate differences in addition to the archaeological fauna (Table 2; Fig. 2).

We sought to obtain rib samples for each individual located in situ at the Cathedral of Santiago's necropolis for paleodietary analysis as good indicators of diet for the last 5–10 years of life (Bartelink and Chesson 2019). However, for some individuals, there was a lack of ribs present or evident taphonomic degradation of the bone. As a result, we were forced to seek other bone elements for some individuals (n = 8) for δ^{13}C and δ^{15}N analysis—a metatarsal, three skull fragments and four teeth (Table 1 and S1). For the tooth dentine and enamel analyses, to avoid breastfeeding influences, we sampled teeth which develop after the first 2 years of life (11 s molars and two premolars). Additionally, according to their availability, we sought to analyse a tooth and rib from the same individual (n = 9), avoiding those teeth that present caries or cavities that could alter isotopic values. Through these two elements, we obtained collagen reflecting the individual's diet during their earlier (tooth) (Wright and Schwarcz 1999) and later years of (rib) of life (Fahy et al. 2017; Hedges and Reynard 2007; Hill 1998). By sampling the tooth enamel δ^{13}C$_{ap}$ as well as the dentine, we can also study the differences between whole diet and protein-based contributions to δ^{13}C, respectively (Fernandes et al. 2012).

For paleomobility, tooth enamel was sampled for δ^{18}O and ^{87}Sr/^{86}Sr analysis (Table 1). This was mostly conducted on the enamel from the same tooth analysed for paleodietary studies. Thus, the palaeomobility dataset was mainly composed of second molars except for two premolars. However, for ^{87}Sr/^{86}Sr analysis, for seven individuals, we took different samples as second molars were not available (e.g. NCS001, NCS006a, NCS011 or NCS034) that still reflected a young age (Table 1). In some individuals (n = 9), the enamel of more than one tooth was sampled to contrast different moments of the individual's early life (Table 1). In total, we sampled 34 human teeth and bones for δ^{13}C and δ^{15}N collagen analysis, and 29 and 33 human teeth for δ^{18}O and δ^{13}C$_{ap}$ and ^{87}Sr/^{86}Sr analysis, respectively.

δ¹³C and δ¹⁵N analysis of bone and tooth collagen

Collagen extraction for δ^{13}C and δ^{15}N analysis was conducted at the Max Planck Geoanthropology (formerly the Max Planck Institute for the Science of Human History),

Table 2 δ^{13}C, δ^{15}N, δ^{18}O$_{ap}$, δ^{13}C$_{ap}$, δ^{18}O$_{dw}$ and ^{87}Sr/^{86}Sr archaeological and modern fauna from Cathedral of Santiago, Rocha Forte Castle, and the city of Santiago de Compostela (CoS=Mediae-val Necropolis Cathedral of Santiago; RF=Rocha Forte Castle; MSS=Modern Snail Santiago de Compostela)

Sample reference	Site	Specie	δ^{15}N and δ^{13}C (‰)	δ^{18}O$_{ap}$ and δ^{13}C$_{ap}$ (‰)	δ^{18}O$_{dw}$	^{87}Sr/^{86}Sr ± 2 s internal
NCS(FAU)01	CoS	*Bos taurus*	4.6 −21.2	-	-	-
NCS(FAU)02	CoS	*Bos taurus*	3.9 −21.6	-	-	-
NCS(FAU)04	CoS	Ovicaprid	5.2 −21.5	-	-	-
NCS(FAU)08	CoS	*Bos taurus*	5.4 −21.3	-	-	-
NCS(FAU)09	CoS	Ovicaprid	4.8 −21.4	-	-	-
NCS(FAU)010	CoS	Ovicaprid	4.9 −21.4	-	-	-
NCS(FAU)012	CoS	*Bos taurus*	4.5 −21.3	-	-	-
NCS(FAU)013	CoS	*Bos taurus*	5.4 −21.3	-	-	-
NCS(FAU)014	CoS	Ovicaprid	5.6 −21.4	-	-	-
UE 2700	CoS (see Fig. 2, #1–3)	*Helix aspersa*	-	-	-	0.712620 ± 12
UE 602	CoS (see Fig. 2, #1–3)	*Helix aspersa*	-	-	-	0.709229 ± 15
UE2700B	CoS (see Fig. 2, #1–3)	*Helix aspersa*	-	-	-	0.712958 ± 14
RF(GAL)FAU01	RF	Ovicaprid	8.8 −22.2	−4.1 −12.3	-6.2	0.711777 ± 12
ROCHA-BOS	RF	*Bos taurus*	5.6 −21.8	-	-	-
ROCHA-SUS	RF	*Sus scrofa*	8.7 −19.6	-	-	-
RF (FAU)MO-25/9	RF	*Bos taurus*	5.9 −22.1	-	-	-
RF (FAU)MO-65	RF	Ovicaprid	5.5 −21.2	-	-	-
RF (FAU)MO-35	RF	Ovicaprid	6.7 −22.3	−3.6 −12.7	-5.4	0.711140 ± 12
MO-65/1	RF	Ovicaprid?	8.8 −21.6	-	-	-
MO-29/4	RF	Ovicaprid	6.9 −22.2	-	-	-
MO-25/7	RF	*Sus Scrofa*	8.5 −19.7	−5.2 −11.3	-8.1	0.715689 ± 10
RF (GAL)FAU069	RF	Ovicaprid	6.2 −22	-	-	-
MO-25/11	RF	*Sus Scrofa*	9.1 −18.5	-	-	-
MO25/10	RF	Ovicaprid	5.0 −21.8	-	-	-
MO61/4	RF	*Bos taurus*?	6.1 −21.8	-	-	-
MO68/4	RF	*Bos taurus*	6.0 −21.9	-	-	-

Table 2 (continued)

Sample reference	Site	Specie	$\delta^{15}N$ and $\delta^{13}C$ (‰)	$\delta^{18}O_{ap}$ and $\delta^{13}C_{ap}$ (‰)	$\delta^{18}O_{dw}$	$^{87}Sr/^{86}Sr$ ± 2 s internal
MO69/8	RF	Ovicaprid	4.7 −21.7	-	-	-
MO-02/1y2	RF	*Merlucciiae*	13.0 −13	-	-	-
MO-44	RF	*Delphinidae*	11.9 −11.9	-	-	-
RF(FAU)MO-69/7	RF	Ovicaprid	-	−5.1 −14.3	-7.9	0.718523 ± 15
RF(FAU)MO-14/2	RF	*Bos taurus*	-	−5.8 −14.7	-9.0	0.713664 ± 34
RF(FAU)MO-68/3	RF	*Equus ferus caballus*	-	−6.0 −13.5	-9.4	0.710225 ± 12
RF(FAU)MO-28/1	RF	Ovicaprid	-	−3.5 −15.2	-5.2	0.715651 ± 13
RF(FAU)MO-14/3	RF	Ovicaprid?	-	−2.1 −14.2	-3.0	0.717897 ± 12
RF(FAU)MO-72/3	RF	*Sus scrofa*	-	−4.6 −8.2	-7.0	0.714961 ± 13
RF(FAU)MO-61/3	RF	Ovicaprid	-	−3.7 −14.3	-5.5	0.716357 ± 18
RF(FAU)MO-44/5	RF	*Cervus elaphus*	-	−5.4 −13.4	-8.4	0.717544 ± 13
RF(FAU)MO-44/6	RF	*Cervus elaphus*	-	−4.5 −13	-6.8	0.718105 ± 10
RF(FAU)MO-68/1	RF	*Sus scrofa*	-	−3.0 −12.4	-4.4	0.713605 ± 15
RF(FAU)MO-68/2	RF	Ovicaprid	-	−2.0 −12.6	-2.8	0.718247 ± 10
RF(FAU)MO-68/3(2)	RF	*Bos taurus*	-	−6.0 −13.5	-9.4	0.711799 ± 12
RF (FAU)MO-69/6	RF	*Bos taurus*	-	−4.7 −12.7	-7.1	0.711799 ± 12
RF (FAU)MO-61/2	RF	*Bos taurus*	-	−5.3 −14.1	-8.2	0.713484 ± 14
RF (FAU)MO-65/5	RF	Ovicaprid	-	−4.0 −14.1	-6.0	0.716870 ± 12
MSS SARELA	MSS (see Fig. 2, #4)	*Helix aspersa*	-	-	-	0.711159 ± 13
MSS ZONE 1	MSS (see Fig. 2, #5)	*Helix aspersa*	-	-	-	0.711239 ± 10
SAN SN1	MSS (see Fig. 2, #6)	*Helix aspersa*	-	-	-	0.711036 ± 11
MSS ZONE	MSS (see Fig. 2, #7)	*Helix aspersa*	-	-	-	0.709364 ± 12
MSS ZONE	MSS (see Fig. 2, #8)	*Helix aspersa*	-	-	-	0.709544 ± 10
MSS ZONE 4	MSS (see Fig. 2, #9)	*Helix aspersa*	-	-	-	0.712407 ± 12
MSS ZONE 5	MSS (see Fig. 2, #10)	*Helix aspersa*	-	-	-	0.712335 ± 14

Jena, Germany. Collagen was extracted following the methodology reported by Richards and Hedges (1999). Bone and root tooth samples (approx. 1 g) were broken into small pieces and any adhering soil was removed by abrasion using a sandblaster. Samples were demineralised by immersion in 0.5 M HCl for ~ 7 days. Once demineralisation was complete, samples were rinsed three times with ultra-pure H_2O. The residue was gelatinised in pH3 HCl at 70 °C for 48 h and the soluble collagen solution Ezee-filtered to remove insoluble residues (Brock et al. 2013). Samples were lyophilised in a freeze dryer for 48 h. Where sufficient material was available, approximately 1.0 mg of the resulting purified collagen weighed in duplicate into tin capsules for analysis. The $\delta^{13}C$ and $\delta^{15}N$ ratios of the bone collagen were determined using a Thermo Scientific Flash 2000 Elemental Analyser coupled to a Thermo Delta V Advantage mass spectrometer. Isotopic values are reported as the ratio of the heavier isotope to the lighter isotope ($^{13}C/^{12}C$ or $^{15}N/^{14}N$) as δ values in parts per mill (‰) relative to international standards, VPDB for $\delta^{13}C$ and atmospheric N2 (AIR) for $\delta^{15}N$. Results were calibrated against international standards (IAEA-CH-6 Sucrose, IAEA-N-2 Ammonium Sulphate and USGS40 L-Glutamic Acid); USGS40 $\delta^{13}C = -26.4 \pm 0.1‰$, $\delta^{13}C = -26.4 \pm 0.0‰$, $\delta^{15}N = -4.4 \pm 0.1‰$, $\delta^{15}N = -4.5 \pm 0.2$; IAEA N2 $\delta^{15}N = 20.2 \pm 0.1‰$, $\delta^{15}N = 20.3 \pm 0.2‰$; IAEA C6 $\delta^{13}C = -10.9 \pm 0.1‰$, $\delta^{13}C = -10.8 \pm 0.0‰$. Replicate analyses of standards suggest that machine measurement error is c. $\pm 0.1‰$ for $\delta^{13}C$ and $\delta^{15}N$. Overall measurement precision was studied through the measurement of repeat extracts from a fish gelatine standard (n = 20, $\pm 0.1‰$ for $\delta^{13}C$ and $\pm 0.1‰$ for $\delta^{15}N$). The atomic C:N ratio along with the collagen yields was used in order to determine the quality of collagen preservation. Collagen yields over 1 wt% were considered acceptable for carbon and nitrogen values (van Klinken 1999), whilst the C:N ratio should have a range from 2.9 to 3.6 (DeNiro 1985).

$\delta^{18}O_{ap}$, $\delta^{13}C_{ap}$ and $^{87}Sr/^{86}Sr$ analysis in tooth enamel and snail shells

Tooth enamel for $^{87}Sr/^{86}Sr$, $\delta^{18}O_{ap}$ and $\delta^{13}C_{ap}$ analysis was removed from clean locations using a tungsten drill, with the vertical edge of the occlusal surface being sampled to provide a long-term average signal. Powdered enamel for $\delta^{18}O_{ap}$ and $\delta^{13}C_{ap}$ analysis was collected and placed in a 1.5-mL Eppendorf tube. Samples were treated with 1 mL of 1% NaClO for 60 min then rinsed with MilliQ water three times to remove any remaining bleach and ultimately treated with 0.1 M acetic acid for 10 min. Again, followed by rinsing three times with MilliQ water to remove any remaining acid. Enamel samples were then covered, frozen and lyophilized for 4 h. From each sample, approximately 3 mg enamel powder was weighed into 12 mL borosilicate glass vials and sealed with

rubber septa. Samples where then flush/filled with helium at 100 mL/min for 10 min. Following reaction with 100% phosphoric acid, gases evolved from the samples were analysed to stable carbon and oxygen isotopic composition using a Thermo Gas Bench 2 connected to a Thermo Delta V Advantage Mass Spectrometer at the Department of Archaeology, Max Planck Institute for the Science of Human History. Stable oxygen ($\delta^{18}O$) and carbon isotope ($\delta^{13}C$) values were calibrated against international standards (IAEA NBS 18, IAEA 603, IAEA CO8) registered by the International Atomic Energy Agency: IAEA NBS 18: $\delta^{13}C - 5.014 \pm 0.032‰$, $\delta^{18}O - 23.2 \pm 0.1‰$; IAEA 603: $\delta 13C + 2.46 \pm 0.01‰$, $\delta^{18}O - 2.37 \pm 0.04‰$; IAEA CO8: $\delta^{13}C - 5.764 \pm 0.032‰$, $\delta^{18}O - 22.7 \pm 0.2‰$ and USGS44: $\delta^{13}C = \sim -42.1‰$. Replicate analyses of standards suggest that machine measurement error is c. $\pm 0.1‰$ for $\delta^{13}C$ and $\pm 0.2‰$ for $\delta^{18}O$. Overall measurement precision was studied through the measurement of repeat extracts from a bovid tooth enamel standard (n = 20, $\pm 0.2‰$ for $\delta^{13}C$ and $\pm 0.4‰$ for $\delta^{18}O$). Human enamel $\delta^{18}O_{ap}$ was converted to $\delta^{18}O_{dw}$ following Chenery et al. (2012) and Daux et al. (2008): $\delta^{18}O_{cVSMOW} = (1.03091 \times \delta^{18}O_{ap}) + 30.91$; $\delta^{18}O_{ap} = (1.0322 \times \delta 18Oc) - 9.6849$; $\delta^{18}O_{dw} = (1.590 \times \delta^{18}O_{cVSMOW}) - 48.634$.

$^{87}Sr/^{86}Sr$ analysis of enamel and snail shells was conducted at the Department of Geological Sciences of the University of Cape Town, South Africa. The sample preparations process varied depending on the material. Snail shells were cleaned and digested. Samples of ca. 20 mg were treated with 2 mL of 65% HNO_3, leaving it in closed Teflon beakers on a hot plate at 140 °C overnight. One millilitre 2 M HNO_3 was added to the samples and placed again on the hot plate at the same temperature. Samples were treated then with 2 mL 2 M HNO_3 and, from this solution, 1.5 mL was centrifuged for 20 min. This 1.5 mL of sample was the solution used to isolate the strontium fraction through chemical separation using 0.2 mL of Sr. Spec resin in Bio-Spin Disposable Chromatography Bio-Rad columns according to the method of Pin et al. (1994). The human and animal tooth enamel samples were digested in HNO_3, calculating the Sr concentration levels for possible diagenesis. After analysing the enamel concentrations, samples were treated following Pin et al. (1994) starting by adding 2 mL of 65% HNO_3. The separated strontium fraction was dried down, dissolved in 2 mL 0.2% HNO_3 and diluted to 200 ppb Sr concentrations for isotope analysis using a Nu Instruments NuPlasma HR MC-ICP-MS. All $^{87}Sr/^{86}Sr$ data are referenced to a value of 0.710255 for bracketing analyses of the international standard SRM987. Instrumental mass fractionation is corrected using the exponential law and a value of 0.1194 for $^{86}Sr/^{88}Sr$. Isobaric interference by Rb at 87 amu is corrected using the measured ^{85}Rb signal and the natural abundance ratio of $^{85}Rb/^{87}Rb$. Background Sr

levels were assessed using total procedural blanks, which averaged < 250 pg Sr and therefore neglectable.

Statistical analysis

Mann–Whitney U ($p_{same-mediane}$) test with a Monte Carlo permutation was applied to $\delta^{13}C$, $\delta^{15}N$, $\delta^{18}O_{ap}$ and $\delta^{13}C_{ap}$ data obtained in this study when comparing differences between two groups.

For several sample tests (3 or more groups), we used the Kruskal–Wallis test for sample comparison followed by a Mann–Whitney pairwise test with a Bonferroni correction. We employed a 5% significance level (α). These tests were used to determine if there were significant differences based on grave location and type, biological sexes, local and no-local individuals identified on the basis of $^{87}Sr/^{86}Sr$ and variations between teeth and ribs from the same individuals (Tab. S4 and S5). We also tentatively convert our $\delta^{18}O_{ap}$ data to $\delta^{18}O_{dw}$ as one way of exploring variation within the dataset, despite the margin of error expected (Evans et al. 2012; Lightfoot and O'Connell 2016). Human enamel $\delta^{18}O_{ap}$ was converted to $\delta^{18}O_{dw}$ following Chenery et al. (2012) and Daux et al. (2008). The resulting data were compared to modern local water values (Araguas-Araguasa and Diaz Teijeiro 2005; http://www.waterisotopes.org) (Fig. S3). In addition to this, we employed two statistical assessments. Boundaries of intra-sample variation based on two measurements of scales were defined: ± 2 standard deviation (2SD) from the mean and Tuke's inter-quartile range method (IQR) considering 1.5xIQR and 3xIQR (Lightfoot and O'Connell 2016). The free software 'PAST' was used for all statistical analyses (Hammer et al. 2001).

Results

Figure 4 and Table S2 display the radiocarbon results for samples dated in this study whilst $\delta^{15}N$, $\delta^{13}C$, $\delta^{18}O$ and $^{87}Sr/^{86}Sr$ results for human and fauna samples can be found in Tables 1 and 2, respectively. $\delta^{13}C$ and $\delta^{15}N$ Incremental Dentine data can be found in Table S1. $\delta^{13}C$ and $\delta^{15}N$ and collagen quality indicators for each analysed sample, as well as the results of the statistical tests, can be found in Tables S3 to S8 in the Supplementary Information. We did not observe a distinction between sexes concerning their grave placement (Fig. 2 and S1; Tab. S4), which rather appears to be associated with socio-economic status. All individuals were buried following the standard Christian rite (east–west orientation, arms stretched out and with the hands over the stomach or pelvis) of the time without evidence for the presence of other faiths.

Faunal $\delta^{15}N$ and $\delta^{13}C$ from collagen and $\delta^{13}C_{ap}$

Stable isotope results for all analysed terrestrial fauna from Rocha Forte Castle (Fig. 6 and 7; Table 2 and S6) ($\delta^{15}N$ and $\delta^{13}C$ n = 15, and C_{ap} n = 18) range between 4.7 and 9.1‰ for $\delta^{15}N$ (Mean ± SD = 6.8 ± 1.5‰), between − 22.3 and − 18.5‰ for $\delta^{13}C$ (mean ± SD = − 21.3 ± 1.1‰) and between − 15.2 and − 8.2‰ for $\delta^{13}C_{ap}$ (Mean ± SD = − 13.1 ± 1.6‰). Statistical testing demonstrates a difference in $\delta^{13}C$ between purely herbivorous domesticated taxa (*Bos taurus* and ovicaprine) and omnivores (*Sus scrofa*) (Mann–Whitney pairwise test with Bonferroni correction p-value < 0.05) (Tab. S7), though there was no difference in $\delta^{13}C_{ap}$ between *Sus scrofa* and *Cervus*

Fig. 6 $\delta^{13}C$ and $\delta^{15}N$ of fauna and humans analysed in the present study and data from marine fauna collected from A Lanzada (López-Costas and Müldner, 2016)

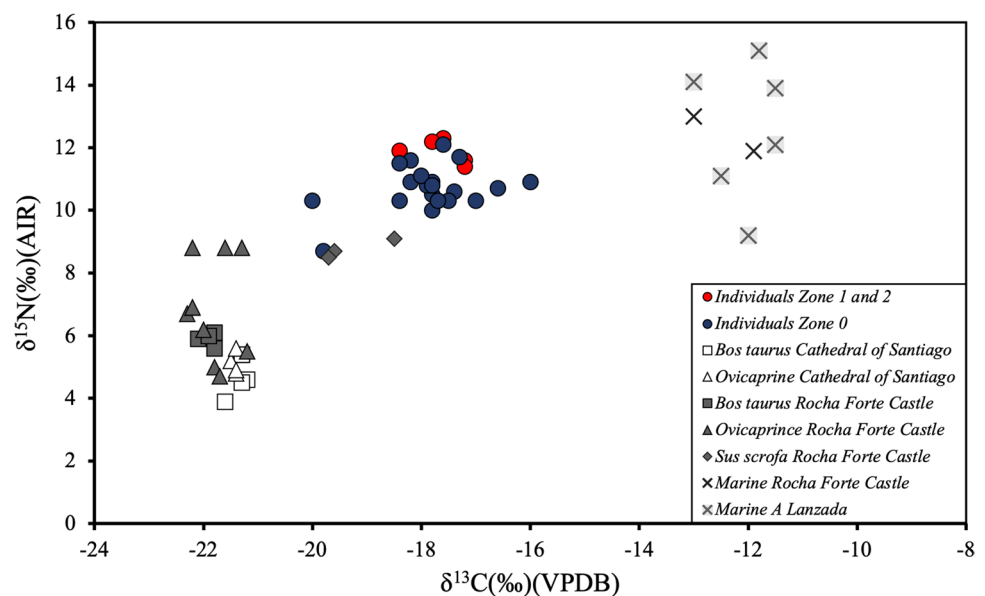**Fig. 7** $\delta^{18}O$ and $^{87}Sr/^{86}Sr$ of archaeological fauna and human tooth enamel and modern snail shells analysed in the present study. The orange zone delimits the local strontium values (modern and archaeological snail shells (with each data point shown with an orange line) from the city's different geographical areas). The blue area indicates Santiago de Compostela's $\delta^{18}O$ values established after individuals identified here as locals via their $^{87}Sr/^{86}Sr$ values
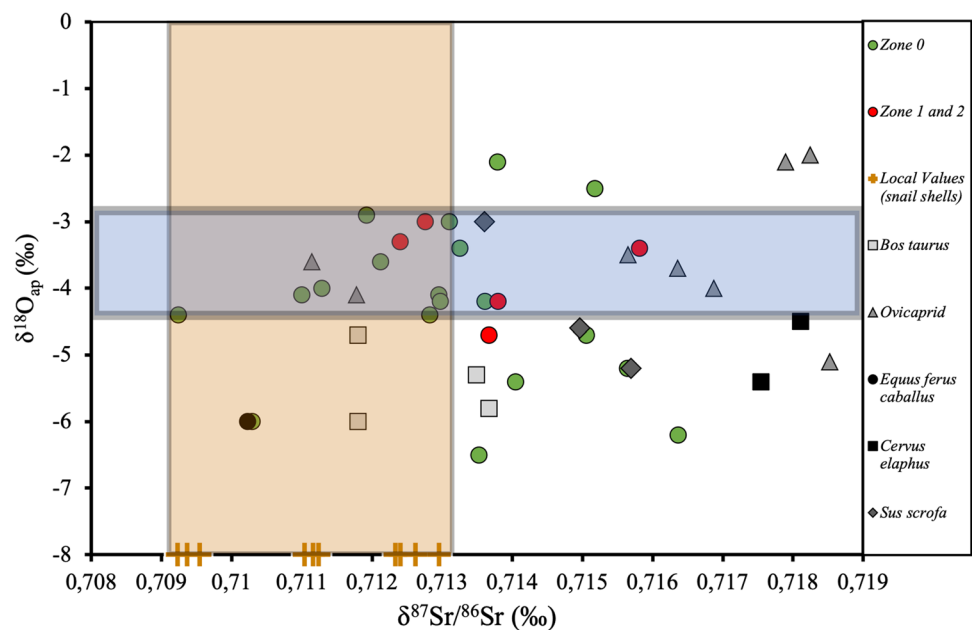
elaphus (Mann–Whitney pairwise test with Bonferroni correction p-value > 0.05) (Tab. S7 and S8).

The collagen values from the terrestrial fauna excavated from the Cathedral of Santiago itself (n = 9) show a $\delta^{15}N$ range from 3.9 to 5.6‰ (mean ± SD = 4.9 ± 0.5‰) and $\delta^{13}C$ range from − 21.6 to − 21.2‰ (Mean ± SD: − 21.4 ± 0.1‰). Overall, the terrestrial fauna excavated from the Cathedral shows lower $\delta^{15}N$ values (Mean ± SD = 4.9 ± 0.5‰) when compared to that from Rocha Forte (Mean ± SD = 6.8 ± 1.5‰), something also seen in *Bos taurus* and *Ovis orientalis aries/Capra aegagrus hircus* identified at both locations (Table 2 and S6). $\delta^{13}C$ differences between the two sites are only observed in *Bos taurus*, however. This is supported by statistical testing which found a significant difference for $\delta^{15}N$ and $\delta^{13}C$ between the terrestrial fauna (*Bos taurus* and ovicaprids) between sites (p < 0.05), and for *Bos taurus* (Mann–Whitney test with Monte-Carlo permutation p-value < 0.05) in particular (Tab. S8).

Human $\delta^{15}N$ and $\delta^{13}C$ from collagen and $\delta^{13}C_{ap}$

The mean $\delta^{15}N$ and $\delta^{13}C$ (‰) of all individuals that we were able to analyse (n = 25) have been obtained from the rib collagen (n = 17), together with the collagen of the dentine (n = 5), and skull fragments (n = 3) from those individuals that we were not able to analyse a rib (n = 8). The human $\delta^{15}N$ and $\delta^{13}C$ data (n = 25) (Table 1 and S3; Figs. 6, 7, S4, and S5) ranges from 8.7 to 12.3‰ for $\delta^{15}N$ (Mean ± SD = 10.9 ± 0.8‰), and from − 20.0 to − 16.0‰ for $\delta^{13}C$ (Mean ± SD = − 17.8 ± 0.8‰). Individuals in zone '0', the largest area of the necropolis and furthest

from the entrances to the original basilica of Alfonso III (Fig. 3), have $\delta^{15}N$ values ranging from 8.7 to 12.1‰ (Mean ± SD = 10.7 ± 0.7‰) and $\delta^{13}C$ values ranging from − 20.0 to − 16.0 (Mean ± SD = − 17.9 ± 0.9‰). By contrast, individuals from zones '1' and '2', areas located at the entrances to the temple of Alfonso III (Fig. 3), with area '2' likely reserved for members of the clergy and other privileged individuals (López Alsina 2015; Guerra Campos 1982; Carro Otero and Varela Ogando 1982), have $\delta^{15}N$ values ranging from 11.4 to 12.3‰ (Mean ± SD = 11.9 ± 0.4‰) and $\delta^{13}C$ values ranging from − 18.4 to − 17.2‰ (Mean ± SD = − 17.6 ± 0.5‰) (Fig. 6). Zones '1' and '2' had significantly (Mann–Whitney test with Monte-Carlo permutation p-value < 0.05) higher $\delta^{15}N$ than zone '0'. No significant difference was found for $\delta^{13}C$ between zone '0' and zones '1' and '2' (Mann–Whitney test with Monte-Carlo permutation p-value > 0.05) (Tab. S4). No statistically significant differences were observed between individuals with different tomb typologies (Kruskal–Wallis test for equal medians p-value > 0.05) (Tab. S5). The $\delta^{13}C_{ap}$ values for human enamel (n = 17) (Table 1; Fig. S5) ranged from − 14.2 to − 6.4‰ (Mean ± SD = − 10.2 ± 2.2‰). $\delta^{13}C_{ap}$ for individuals from Zone '1' and '2' ranged between − 14.2 and − 8.7 (Mean ± SD = − 11.3 ± 2.3‰) compared to − 13.7 to − 6.4 (Mean ± SD = − 10.1 ± 2.3‰) for Zone '0'. No statistically significant difference was observed for $\delta^{13}C_{ap}$ (Mann–Whitney test with Monte-Carlo permutation p-value > 0.05) (Tab. S4).

For nine individuals, tooth dentine and rib samples were taken from the same individual for $\delta^{15}N$ and $\delta^{13}C$ analyses. The teeth showed $\delta^{15}N$ values ranging from 10.4 to 12.7‰ (Mean ± SD = 11.2 ± 0.8‰) and $\delta^{13}C$ between − 17.8

and $-15.5‰$ (Mean $\pm$ SD $= -16.5 \pm 0.9‰$). Meanwhile, ribs showed $\delta^{15}N$ values between 10.3 and 12.1‰ (mean and SD: $10.9 \pm 0.6‰$) and $\delta^{13}C$ values between -18.2 and $-16.6‰$ (Mean $\pm$ SD $= -17.6 \pm 0.4‰$). Comparison of isotopic values between collagen from different elements can be challenging as variable fractionation is expected depending on the skeletal element, with lower $\delta^{15}N$ being identified in tissues with a high rate of bone remodelling (e.g. rib or metacarpals) for example (Fahy et al. 2017). However, overall comparison of $\delta^{13}C$ and $\delta^{15}N$ from rib collagen (formed during last 10–15 years of life) (Fahy et al. 2017) and dentine collagen (formed during the period of tooth formation) should provide broad insights into diet during different periods of life (Beaumont et al. 2015). A comparison between tissues illustrated that there was a significant (Mann–Whitney test with Monte-Carlo permutation p-value < 0.05) difference in $\delta^{13}C$ between the tissues, although no statistically significant differences were found for $\delta^{15}N$ (Fig. S4 and S5; Tab. S4). We also compared the $\delta^{15}N$ and $\delta^{13}C$ data by the estimated sex of the skeleton. Female individuals (n = 10) have $\delta^{15}N$ values of 10.0 to 12.1‰ (Mean $\pm$ SD $= 10.7 \pm 0.6‰$) and $\delta^{13}C$ between -18.4 and $-16.6‰$ (Mean $\pm$ SD $= -17.7 \pm 0.5‰$). Male individuals (n = 9) showed $\delta^{15}N$ values from 10.3 to 12.3‰ (Mean $\pm$ SD $= 11.2 \pm 0.6‰$) and $\delta^{13}C$ between -20 and $-16‰$ (Mean $\pm$ SD $= -17.9 \pm 1.1‰$). Female $\delta^{13}C_{ap}$ values are from -12.8 to $-6.4‰$ (Mean $\pm$ SD $= -10.2 \pm 2.4‰$) and male $\delta^{13}C_{ap}$ ranges between -13.0 and $-6.9‰$ (Mean $\pm$ SD $= -9.8 \pm 2.6‰$). No statistically significant differences were observed between sexes for any of the isotopic proxies (Tab. S4).

Fauna and human $^{87}Sr/^{86}Sr$ and $\delta^{18}O_{ap}$ data

The most appropriate method for establishing a local bioavailable Sr isotopic signature for a given past site is still the subject of an ongoing debate that has occurred over the last few decades without clear consensus (Larsson et al. 2020; Scaffidi et al. 2020; Grimstead et al. 2017). Unfortunately, Santiago de Compostela's underlying bedrock geology is highly variable even over short distances, and the geological substrate is heterogeneous (Fig. 2). Variation in local growing conditions and the underlying geological variability of Santiago de Compostela would necessitate a widespread sampling strategy to produce an appropriate Sr baseline (Britton et al. 2020). Many scholars have recently argued that the preferred method to define a local $^{87}Sr/^{86}Sr$ range is to analyse surface waters, soils, plants and archaeological fauna in the locality of a given site (Larsson et al. 2020; Grimstead et al. 2017). However, Holt et al. (2021) described the use of plants for mapping strontium ratios as problematic because of the point-bias, a consequence of the idiosyncrasies of geological and environmental processes. Therefore, a

single plant may show a ratio that is not representative of the area where it grows. This can only be solved by the analysis of a large number of samples, something difficult as a result of the significant costs involved (Holt et al. 2021). Besides, the $^{87}Sr/^{86}Sr$ ratios may vary between plants based on the type and area of their roots (Britton et al. 2020; Hartman and Richards 2014), local environmental factors such as soil types, precipitation regimes (Holt et al. 2021) and wind-blown dust (Blank et al. 2018). Another method that may not reflect terrestrial bioavailable strontium as closely as other archives is water (Hartman and Richards 2014; Hamilton et al. 2019). This, together with other approaches as soil and plants, may be affected by anthropogenic activities (Holt et al. 2021). The use of fertilisers, nutrients, plants cultivated elsewhere (e.g. urban parks) or indirect alterations such as contamination may lead to unrepresentative local bioavailable Sr isotopic signatures when compared to the past (Holt et al. 2021; Casado et al. 2019).

The Cathedral of Santiago de Compostela is located in the modern city centre. Thus, the study area is today fully urbanised. Moreover, the water in Santiago de Compostela has very serious pollution problems (Suárez et al. 2009; Alertan… 2006) that can impact the $^{87}Sr/^{86}Sr$ ratios (Casado et al. 2019). Therefore, in order to establish the best baseline available possible, we first sought to analyse the archaeologically available domestic fauna, from the Cathedral itself and nearby Rocha Forte Castle, as better integrators of locally available bioavailable strontium sources for humans in the past (Holt et al. 2021; Adams et al. 2019). This proved difficult as faunal teeth were only available from the Rocha Forte Castle which is located some distance from the Cathedral and dates to a later time period when fauna could be arriving from outside of the local area given the position of the castle which sat at the node of trade routes during the 13th and 15th centuries AD (López-Costas and Teira Brión 2014). Consequently, we also decided to establish another bioavailable $^{87}Sr/^{86}Sr$ dataset using modern and archaeological wild snails collected across the city following the variation in its geological substrate and those discovered at the mediaeval necropolis of Santiago de Compostela (9th–12th centuries AD), respectively (Table 2; Fig. 2).

Snails, after plants, are recommended by many researchers as having $^{87}Sr/^{86}Sr$ values that broadly correspond with the lithological unit/soil values of various square metres over a few years and are more likely to integrate a wider geographical range (Blank et al. 2018; Britton et al. 2020; Holt et al. 2021). However, some scholars have debated the feasibility of using snail shells to develop an isoscape. Hartman and Richards (2014) suggested that their $^{87}Sr/^{86}Sr$ ratios map shallow-rooted plants more closely, as opposed to deep-rooted plants. Moreover, as with plants or soil, snail shells can yield $^{87}Sr/^{86}Sr$ ratios strongly affected by rainwater (Evans et al. 2010). Given the complexity of the

task, to ensure the viability of the method used, we also compared the strontium isotope composition of our modern local (n=7) and archaeological (n=3) snail shells, which range between 0.709229 and 0.712958 (Table 2; Fig. 2). This range is expected based on the underlying bedrock from the closets sites analysed (Voerkelius et al. 2010; Bea et al. 2003; James et al. 2022; Waterman et al. 2014) with the Lower Palaeozoic materials having $^{87}Sr/^{86}Sr$ values closer to marine values (oceanic water analysis has $^{87}Sr/^{86}Sr$ ranging between 0.709 and 0711) (Voerkelius et al. 2010), whilst the Hercynian granitic rocks from the Iberian Peninsula interior are expected to have more radioactive values approaching 0.713 (Bea et al. 2003; James et al. 2022; Waterman et al. 2014).

The $^{87}Sr/^{86}Sr$ ratios measured on human remains within the necropolis of the Cathedral (n=26) span between 0.709236 and 0.716632 (Fig. 7; Table 1). Female individuals (n=8) have $^{87}Sr/^{86}Sr$ values from 0.709236 to 0.713785, and male individuals (n=9) have values of $^{87}Sr/^{86}Sr$ ranging between 0.710287 and 0.716632. A comparison between the modern and archaeological snail shells and the human data obtained suggests that 14 of the 26 individuals for which $^{87}Sr/^{86}Sr$ data was available could be identified as non-local (Fig. 7; Table 1). Although some fauna from the Rocha Forte Castle are also consistent with the local Santiago range (0.709229 to 0.712958) based on our analysis of snails and predicted values based on the underlying bedrock, the range of faunal $^{87}Sr/^{86}Sr$ from this site (from 0.710225 to 0.718523 (Fig. 7; Table 2) suggests that some of the fauna were non-local (e.g. RF(FAU)MO-69/7: 0.718523; RF(FAU)MO-14/3: 0.717897 or RF(FAU)MO-44/6: 0.718105). Interestingly, some of these potential non-local faunas overlap with the range of variation seen amongst non-local humans. For some human individuals, where we were able to analyse more than one tooth to compare different moments of their childhood (n=9), we found that, in three cases (NCS039: $RP^1/15$ 0.713102 and $RM^2/17$ 0.712937; NCS145a: $LM_1/36$ 0.713797 and $LM_2/37$ 0.711426 and NCS258b: $RM_2/47$ 0.713665 and $RM_3/48$ 0.712886), their values demonstrated variation that is consistent with a non-local origin followed by early immigration to Santiago (Table 1).

$\delta^{18}O_{ap}$ was used to complement the interpretation of the data obtained through strontium isotope analysis. The $\delta^{18}O_{ap}$ values of the fauna analysed from Rocha Forte Castle (n=18) range between −6.0 and −2.0‰ (Mean ± SD = −4.4 ± 1.2‰) (Table 2), within the range of variation expected for a single site or locale (Britton et al. 2020). $\delta^{18}O_{ap}$ values for humans (n=17) from the mediaeval necropolis ranged from −6.5 to −2.1‰ (Mean ± SD = −4.0 ± 2.2‰) (Table 1). Zone '0' (n=13) $\delta^{18}O_{ap}$ spans from −6.5 to −2.1‰ (Mean ± SD = −4.0 ± 1.1‰) whilst Zone '1–2' (n=4) $\delta^{18}O_{ap}$ ranges between −4.7 and −3.0‰

(Mean ± SD = −3.8 ± 0.8‰). Female individuals (n=6) have values of $\delta^{18}O_{ap}$ ranging −4.4 to −2.1‰ (Mean ± SD = −3.4 ± 0.9‰), and male individuals (n=5) showed values of $\delta^{18}O_{ap}$ ranging from −5.4 to −3.0‰ (Mean ± SD = −4.2 ± 0.9‰). The $\delta^{18}O_{ap}$ of individuals identified as 'local' based on $^{87}Sr/^{86}Sr$ (n=8) is tighter ranging from −4.2 and −2.9‰ (Mean ± SD = −3.6 ± 0.6‰), whilst 'non-locals' (n=9) range from −6.5 to −2.1‰ (Mean and SD: −4.5 ± 1.4‰) (Tab. S4).

The conversion of our $\delta^{18}O_{ap}$ values to $\delta^{18}O_{dw}$ and their comparison with the modern local water values (−5 ± 2‰) (Voerkelius et al. 2010) (Fig. S3) allow us to identify 4 human individuals (NCS002: $LM_2/37 = −5.4$; NCS025: $LM_3/38 = −6.2$; NCS032: $LP^2/25 = −6.5$ and NCS258b: $RM_2/47 = −4.7$) that potentially come from outside of the region. However, using the ± 2 standard deviation (2SD) from the mean and Take's interquartile range method (IQR) approaches, considering 1.5xIQR and 3xIQR (Lightfoot and O'Connell, 2016), we were only able to identify two human individuals (NCS032 and NCS025) as potentially growing up elsewhere. These are the only two individuals where both methods ($\delta^{18}O_{ap}$ and $^{87}Sr/^{86}Sr$) converge on identifying them as 'non-locals'. No statistically significant differences were observed between zones or sex for $\delta^{18}O_{ap}$ (Mann–Whitney test with Monte-Carlo permutation p-value > 0.05) (Tab. S4). There were also no statistically significant differences observed for local and non-local individuals, identified on the basis of $^{87}Sr/^{86}Sr$, in terms of $\delta^{18}O_{ap}$ (Mann–Whitney test with Monte-Carlo permutation p-value > 0.05) (Tab. S4).

Discussion

From the locus sanctus to the civitas

Our results show a more intense and complex use of the space at the site of the Cathedral than was previously determined through archaeological investigations in the mid-20th century (Chamoso Lamas 1957; Guerra Campos 1982). Overall, the archaeological context and the radiocarbon dating results suggest that there was reutilisation of, and changes in, the original position of most of the tombs related to the first temple (Sarcophagus tombs) (Fig. 3, 4, 5, and S1). This could be a consequence of the continuous alteration of the burial layouts with the construction of successive temples and/or reconstruction after the attacks of Almanzor (Chamoso Lamas 1957; Guerra Campos 1982; López Alsina 1990). In addition, the expansion of the graveyard from the second half of the 11th century AD destroyed the first domestic buildings of the original city centre (Chamoso Lamas 1957; Guerra Campos 1982; López Alsina 1990) (Fig. 3 and S1) and led to the superposition of more recent tombs (tombs type 'Rectangular'), over the previous

ones (sarcophagus, cists and anthropomorphic tombs) (e.g. NCS014 and NCS034), with the appearance of a second, and even a third, level of graves (Figs. 3, 5, and S1).

A city made by immigrants

Based on the snail shells analysed from Santiago de Compostela's different geographical substrate zones, we tentatively determined that $^{87}Sr/^{86}Sr$ local bioavailable values range between 0.709229 and 0.712958 (Fig. 7; Table 2). Based on these parameters, 14 of 26 human individuals analysed can be classified as non-local to the Santiago settlement area (Tables 1 and 2; Fig. 7). This suggests that a significant number of individuals were moving into Santiago following childhood. Notably, however, a number of the fauna sampled from Rocha Forte Castle also appear to be 'non-local' using these parameters, with the exception of two ovicaprines, one *Equus ferus caballus*, and two *Bos taurus* (Table 2). This could indicate that much of the 'non-locality' seen amongst the human individuals is a product of the consumption of animal resources coming from elsewhere (NCS009 and NCS030) as part of an urban network. Santiago de Compostela of the 9th century AD was a collection of buildings of a religious nature that emerged around the apostolic tomb (López Alsina, 2015). Thus, a high degree of non-locality (at least away from the immediate central area) is expected for individuals buried at the site during this time. Nine of 12 individuals that have shown $^{87}Sr/^{86}Sr$ values defined here as 'non-local' were buried in tombs type 'Sarcophagus' (n = 5) and 'Cists' (n = 4), which, according to the ^{14}C results, correspond to the first settlers buried between the 9th and 10th centuries AD, and 10th and 11th AD, respectively (Figs. 3, 5, and S1; Table 1 and S2).

The nucleus of Santiago de Compostela progressively acquired urban characteristics, particularly during the 11th century AD (López Alsina 2015). From at least the eleventh century AD onwards, Santiago de Compostela grew as a trade centre (López Alsina 2015), in parallel with urban developments across northern Iberia more generally at this time (Martínez García 2004; Passini 1993). It is only in the second half of the 11th century that widespread exchange in animals across great distances is likely to have become routine for individuals living in and around Santiago de Compostela, with the potential that external food sources could have perhaps become consistent enough to supply the city and its inhabitants (López Alsina 2015). Rocha Forte Castle's fauna is witness to this, highlighting Santiago de Compostela's relevance as a commercial centre at the end of the Middle Ages. Here, $\delta^{15}N$ and $\delta^{13}C$ variation within the Rocha Forte Castle fauna itself ($\delta^{15}N$ 6.2 ± 1.6‰; $\delta^{13}C$ − 21.4 ± 0.9‰) contrasts that of the earlier Cathedral fauna from the 9th–11th centuries AD ($\delta^{15}N$ 4.9 ± 0.5‰; $\delta^{13}C$ − 21.3 ± 0.1‰), suggesting a growing appearance of

animals raised in regions with different soils, manure inputs, climates and latitudes or altitudes (Drucker 2008; Männel et al. 2007). Indeed, what seems more probable is that the mobility observed in the human population at the founding of Santiago was part of an increasingly solidified network of trade as time went on, with an exchange in animals being built upon earlier movements of people to this site of increasing cultural and political importance.

The $^{87}Sr/^{86}Sr$ values, between 0.714730 and 0.716632, observed in several human individuals from Santiago de Compostela (NCS002, NCS024a, NCS025, NCS026 or NCS033) that fall outside the immediate 'local' range we defined on the basis of mollusc shells are found across large areas of the western half of the Iberian Peninsula, including the northwestern region surrounding Santiago de Compostela, following the models of Hoogewerff et al. (2019) and Bataille et al. (2020) as well as those provided by Díaz-Zorita Bonilla et al. (2018) from La Pijotilla, Badajoz (0.714175–0.715382) (Fig. 1; Tab. S9). Several of the individuals with these values were buried in graves type 'Sarcophagus' (NCS024a, NCS025 and NCS026), probably the first settlers of the new religious centre (NCS023: 769–891 cal AD; NCS146: 772–954 cal AD). Furthermore, individuals NCS010, NCS016, NCS022, NCS032, NCS039, NCS154a and NCS258b yielded $^{87}Sr/^{86}Sr$ values between 0.713525 and 0.713785, fitting with those from Bolores, Extremadura (Portugal) (0.7090750–0.713280) (Waterman et al. 2014), or the Madrid Region (0.707 to 0.713) (Díaz-del-Río, 2017) (Tab. S9). Interestingly, as it has been noted historically (Martínez Díez 2011; Molénat 2019; Cenname 2016), between the 9th and 10th centuries AD, the northern peninsular area corresponds to the kingdom of Asturias which became a refuge for Christians, especially clergymen, who fled from areas dominated by Islamic political powers. This data may highlight that some of these supposedly 'non-local' individuals from between the 9th and 10th centuries AD were, in fact, a product of populations coalescing at a growing socio-economic centre, rather than being 'pilgrims' from distant areas.

This is further supported by the observable non-locality in most $\delta^{18}O_{ap}$ human values obtained (except for NCS032 and NCS025). The oxygen isotopic data reveals that the potential 'non-locals' identified by strontium previously lived in a region with similar environmental conditions to those seen in Santiago of Compostela, suggesting potential provenance from the wider Galicia region and/or other parts of the Kingdom of Asturias. Such an interpretation is complemented by historical sources that suggest that the first portions of the Santiago urban population came from regional rural nuclei (López Alsina 2015). However, as was described above, historical sources also described the potential presence of individuals from across the Iberian Peninsula and even further: references about the presence

of 'Franks' in Santiago de Compostela are from at least the first half of the 10th century AD (López Alsina 2015; Pallares Méndez and Portela Silva 1975). Comparison of our $\delta^{18}O_{ap}$ data (Mean $\pm$ SD $= -4.0 \pm 1.0\%o$; range: -6.5 to $-2.1\%o$) with the data obtained at the nearby Cathedral of Lugo (Mean $\pm$ SD $= -3.6 \pm 1.1\%o$; range: -5.6 to $-2.2\%o$) (López-Costas et al. 2021) shows that the values obtained in Santiago de Compostela are slightly lower, but also suggest the presence of individuals from outside the region. López-Costas et al. (2021) identified an individual (CP-704; $\delta^{18}O_{ap} = -5.6\%o$) that seems to have spent some of his life in the centre of the Iberian Peninsula. Interestingly, this value is closer to those observed in three individuals identified here as potential non-locals (NCS002 $= -5.4\%o$; NCS025 $= -6.2\%o$ and NCS032 $= -6.5\%o$). Perhaps, these three potential non-local individuals were Christian coming from the wider kingdom of Al-Andalus. Although intriguing, geographical pinpointing is challenging if not impossible with $^{87}Sr/^{86}Sr$ analysis and interpretations should remain cautious in this regard.

Some of the tombs analysed contained the remains of more than one individual, something unexpected given known Church prohibitions on this practice (López Quiroga 2018). This practice was especially intensive for tomb type 'Sarcophagus', where 4 of 5 of those sarcophaguses had a minimum number of two individuals. On the basis of $^{87}Sr/^{86}Sr$ from those individuals, 6 of 8 corresponded to potential 'non-locals' (Table 1). Interestingly, 2 of those graves have a 'local' and a 'non-local' individual inside (Table 1). The use of a tomb by more than one individual over time may occur because it was a family grave (members of the same family but from different generations), a burial condition based on marriage (where one individual was from outside Santiago de Compostela), or a grave occupied by non-related individuals that reused the tomb because of the lack of space (e.g. NCS001). Further DNA analysis is needed to test between these hypotheses. Amongst individuals in type 'Sarcophagus' tombs, some of them illustrate an early change of residence. NCS145a could be a possible 'non-local' individual as suggested by the $^{87}Sr/^{86}Sr$ values obtained from the first molar ($^{87}Sr/^{86}Sr = 0.713797 \pm 0.0000014$)—crown enamel development between birth and 2.5–3 years (AlQahtani et al. 2010), moving to Compostela at an early age on the basis of results from its second molar ($^{87}Sr/^{86}Sr = 0.711426 \pm 0.0000010$)—crown enamel second molar development between 2.5 and 7.5 years (AlQahtani et al. 2010) (Table 1). Additionally, another two individuals, NCS039 and NCS258b, also showed $^{87}Sr/^{86}Sr$ variations between teeth, with 'non-local' values during the early years of life (NCS039: RP1/15 $= 0.713102 \pm 0.0000011$—crown enamel developed of the first premolar developing between 2.5 and 6.5 (AlQahtani et al. 2010), and RM2/17 $= 0.712937 \pm 0.0000013$);

NCS258b: RM2/47 $= 0.713665 \pm 0.0000013$, and RM3/48 $= 0.712886 \pm 0.000009$ (Table 1), crown enamel developed of the third molar developing between 8.5 and 12.5 years (AlQahtani et al. 2010). Further analysis may help to explore the patterns of mobility to the city as part of its growing rise to prominence between the 9th and 12th centuries AD.

Diet and social status at the centre of pilgrimage

Mediaeval historical records provide broad expectations in terms of variation in diet types and sources in Iberia as well as their relationship to social status and historical and geographical context. The diets of the social and economic elites throughout the Iberian Middle Ages were primarily characterised by the significant consumption of meat (Jiménez-Brobeil et al. 2016; Pérez-Ramallo et al. 2022; Pérez Samper 2019). Meat, together with dairy products, was available on a more limited basis for most of the rural populations (Pérez-Ramallo et al. 2022; Pérez Samper 2019; Grau-Sologestoa 2017). Peasants were historically distinguished by diets focus on local cereal crops, which vary by region as well as between rural and urban contexts (Peña-Chocarro et al. 2019; Rosener 1992). Following historical and archaeological sources, rye was the most cultivated cereal across Iberia, with wheat preferred as a 'luxury' crop by the social and economic elites (Andrade Cernadas 2009). By contrast, individuals of lower social status, in some parts of Iberia, could also resort to the C_4 crop millet, particularly in years of poor harvests or famine, which was usually reserved for animal fodder (Peña-Chocarro et al. 2019; Grumett and Muers 2010). The pattern of dietary changes in the incremental dentine $\delta^{15}N$ and $\delta^{13}C$ profiles for NCS006 and NCS007 (Fig. S2) may reflect such short-term changes. However, religious dietary restrictions affected all social status groups. Christianity forbade meat consumption during certain fasting dates, which could be as high as 150 days per year involving the consumption of alternative protein sources (marine or freshwater fish, legumes, nuts or vegetables), varying in quantity and quality between individuals (Pérez Samper 2019; Andrade Cernadas 2009; Adamson 2004; Grumett and Muers 2010).

The local fauna analysed from the Cathedral of Santiago and the Rocha Forte Castle demonstrated diets dominated by C_3 plant foods. Distinctions in $\delta^{15}N$ were found between pure herbivores (*Bos taurus* and ovicaprines) and omnivores (*Sus scrofa*), as expected. Lower $\delta^{15}N$ and higher $\delta^{13}C$ were noted for fauna excavated from the Cathedral of Santiago when compared to Rocha Forte castle, perhaps explained by chronological or spatial divergences in environment, agricultural changes or distinctions in food provisioning between the occupants of the castle and the rest of the city as noted above (Hamilton and Thomas 2012). The faunal

data provides a useful baseline for interpreting the human data from the Cathedral complex itself. Human $\delta^{13}C$ and $\delta^{15}N$ values suggest diets mainly based on C_3 foods, but with varying inputs of higher trophic level foods, C_4 plants (e.g. millet) and/or marine or freshwater proteins depending on the individual sampled. Where $\delta^{13}C_{ap}$ enamel and collagen $\delta^{13}C$ and $\delta^{15}N$ were available for the same individual, we can tentatively distinguish individuals with diets rich in C_4 plants (NCS007, NCS009, NCS016, NCS022 and NCS032) to those with significant marine protein inputs (NCS002, NCS003, NCS145b and NCS154) (Table 1; Fig. 6, S4, and S5).

Significantly, variation in diet between individuals is correlated with tomb location. We found a higher apparent consumption of animal and/or aquatic protein in those individuals (NCS154, NCS256, NCS258a, NCS258b and NCS259) buried closer to the entrances of Alfonso III's Basilica (Zones '1' and '2' Mean and SD = $\delta^{15}N$ 11.9 ± 0.4‰, and $\delta^{13}C$ − 17.8 ± 0.9‰) (Fig. 3) that are expected to represent individuals of higher socio-economic status given the location of their graves and additional contextual information (López Alsina 2015, 1990; Guerra Campos 1982; López Quiroga 2018). This fits with existing historical records that document that the diet of the social elite throughout the Middle Ages was primarily characterised by the significant consumption of meat and fish (Jiménez-Brobeil et al. 2016; Pérez-Ramallo et al. 2022). By contrast, individuals found in zone '0' (Mean and SD = $\delta^{15}N$ 10.7 ± 0.7‰, and $\delta^{13}C$ − 17.8 ± 0.9‰), the area with the largest number of burials and located at some distance from the entrances of the Basilica of Alfonso III, indicated a lower consumption of animal protein, a greater divergence in their values and increased presence of C_4 plant inputs to the diet (NCS007, NCS009, NCS016, NCS022 and NCS032) (Fig. 6, S4, and S5). Notably, as it was described above, C_4 crops, such as millet, were generally seen as 'fallback' foods for poorer communities during this period in Iberia (Andrade Cernadas 2009; Peña-Chocarro et al. 2019).

Comparison between teeth and ribs from the same individuals (n = 9) within zone '0' reveals that their diets may have changed over the course of their lives, with C_4 plants and/or marine proteins being replaced by a growing reliance on C_3 food resources, perhaps as a consequence of moving to Santiago de Compostela (Fig. S4). We must remain cautious as comparisons between different bone elements can be influenced by metabolic variations in routing (Fahy et al. 2017); however, clear observed changes can be seen in individuals NCS003, NCS007, NCS009, NCS010 and NCS032 (Fig. S4), and where available in the incremental dentine $\delta^{15}N$ and $\delta^{13}C$ profiles (Fig. S2). Individuals NCS007, NCS009 and NCS010 (from between the 10th and 11th centuries AD) show values that suggest a shift from C_4 to C_3 proteins. By contrast, individuals NCS003

and NCS032 illustrate values that indicate a substitution of marine proteins for terrestrial C_3 inputs. Both correspond to the last phase of occupation of the necropolis (11th–12th centuries AD). Interestingly, only two individuals were identified here as potential non-locals (NCS010 and NCS032) (Table 1). The dietary variation in these two individuals may therefore be a result of geographic mobility. However, individuals NCS007, NCS009 and NCS003 may have responded more to socio-economic changes linked to the possibilities offered in this first mediaeval Galician city. In addition, short geographical mobility from nearby populations with similar geographical or climatic characteristics to those observed in Santiago de Compostela could also explain these variations observed in NCS007, NCS009 and NCS010. In case of NCS007, this individual might be also showing short-term famine and millet consumption (Tab. S1; Fig. S2). Nevertheless, we must remain cautious with this until further analyses are conducted because of the difficulties and limits to establishing an adequate isoscape and a local baseline.

Comparison with published data

Comparison of our new dataset with data from other mediaeval Christian sites (8th to 15th century AD) from northern Iberia available in the literature illustrates the economic and dietary complexity of the society that emerged in Santiago de Compostela between 9th and 12th centuries AD (Fig. 8; Tab. S10). Whilst direct comparison is difficult due to environmental, geographical and temporal differences that impact food isotopic values, the datasets chosen to occur in regions have similar rainfall, soils and temperatures today (MacKinnon et al. 2019; Lubritto et al. 2017; Guede et al. 2018). In this context, there are some differences between human $\delta^{13}C$ and $\delta^{15}N$ from Santiago and other mediaeval Christian communities such as Chao San Martín, San Pedro de Noras, San Salvador de Valdedios, San Miguel de Lillo (MacKinnon et al. 2019), Zaballa, Dulantzi, Aistra, Zornoztegi (Lubritto et al. 2017) and Treviño (Guede et al. 2018). Overall, these other sites have mean $\delta^{15}N$ and/or $\delta^{13}C$ values that are generally lower than those measured at Santiago (Mean and SD = $\delta^{15}N$ 10.9 ± 0.8‰, and $\delta^{13}C$ − 17.8 ± 0.8‰), suggesting greater access to animal protein and/or marine proteins at the latter (Fig. 8; Table 1, and S10): San Salvador de Valdedios (Mean and SD = $\delta^{15}N$ 9.7 ± 0.8‰, and $\delta^{13}C$ − 19.0 ± 0.8‰); Zaballa (Mean and SD = $\delta^{15}N$ 9.4 ± 1.3‰, and $\delta^{13}C$ − 19.9 ± 0.9‰); Dulantzi (Mean and SD = $\delta^{15}N$ 9.1 ± 1.2‰, and $\delta^{13}C$ − 18.8 ± 1.4‰); Aistra (Mean and SD = $\delta^{15}N$ 8.0 ± 1.1‰, and $\delta^{13}C$ − 18.9 ± 1.0‰); Zornoztegi (Mean and SD = $\delta^{15}N$ 8.0 ± 0.6‰, and $\delta^{13}C$ − 18.2 ± 0.8‰) or Las Gobas (Mean and SD = $\delta^{15}N$ 8.9 ± 0.9‰, and $\delta^{13}C$ − 19.0 ± 0.6‰). However, these differences are smaller for the towns closest to Santiago de Compostela: Chao San Martín (Mean and SD = $\delta^{15}N$ 10.1 ± 0.6‰,

Fig. 8 δ^{13}C and δ^{15}N of fauna and humans analysed in the present study compared to compiled literature data (see Table S9)
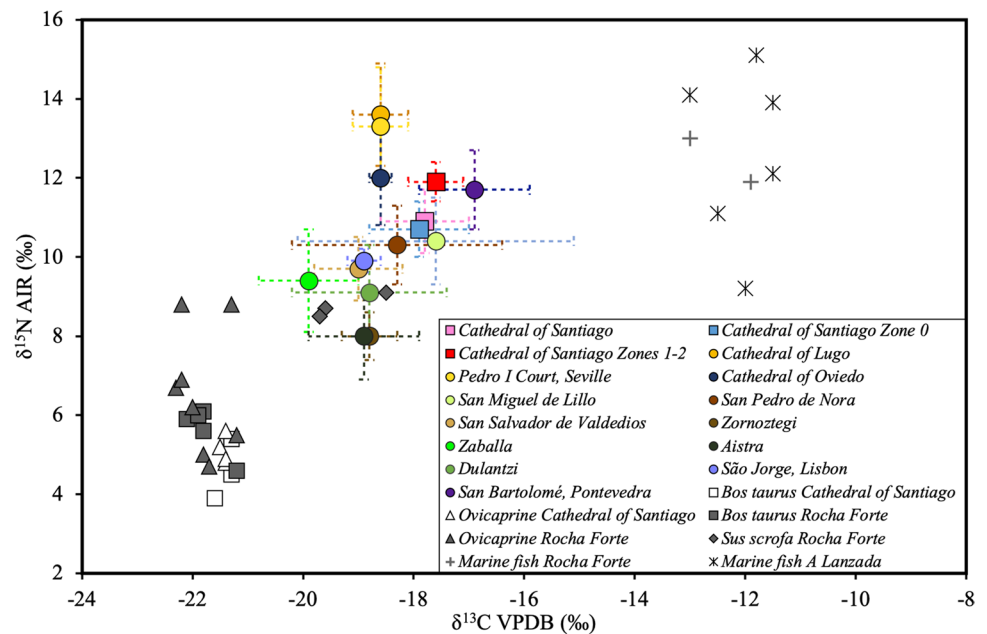
and δ^{13}C − 18.8 ± 0.5‰); San Pedro de Nora (Mean and SD = δ^{15}N 10.3 ± 1‰, and δ^{13}C − 18.3 ± 1.9‰) and San Miguel de Lillo (Mean and SD = δ^{15}N 10.4 ± 1.1‰, and δ^{13}C − 17.6 ± 2.5‰) (MacKinnon et al. 2019). These sites with values closer to those observed in Santiago de Compostela lack of an absolute chronology that makes it difficult to define possible temporal differences. However, it is likely that these sites were influenced by the growing socio-economic sphere of the Santiago via the expanding Camino de Santiago network, with these towns potentially gaining a share in access to the resources being channelled towards this new religious centre (MacKinnon et al. 2019).

Nearby urban centres geographically and/or temporarily such as Pontevedra (López-Costas and Müldner 2018) or Lisbon (Toso et al. 2019) reveal interesting differences that could be because of temporal or religious variations. The adult Muslim individuals analysed from the São Jorge Castle in Lisbon (Mean and SD = δ^{15}N 9.9 ± 0.8‰, and δ^{13}C − 18.9 ± 0.3‰), even though they could be members with a high social status, show values below those of Santiago de Compostela. However, the individuals from San Bartolomé in Pontevedra (Mean and SD = δ^{15}N 11.7 ± 1.0‰, and δ^{13}C − 16.9 ± 1.0‰) show higher nitrogen and carbon isotope values, possibly the product of a diet with strong contributions of marine protein given their easy access to the coast (López-Costas and Müldner 2018). Comparison with known high-status individuals such as the King Pedro I and his court (the analysed individuals lived in the north but were buried in Seville; 14th century AD) (Jiménez-Brobeil et al. 2016) or priests of high status at Capela do Pilar, Lugo (14th–15th centuries AD) (López-Costas et al. 2021; Kaal et al. 2016); San Salvador Cathedral, Oviedo (10th century

AD) (MacKinnon et al. 2019), shows that the Santiago community as a whole did not reach these levels of access to high trophic foods, although in individuals from Zones '1' and '2', the differences are smaller (Figs. 6 and 8; Table 1 and S10). However, over environmental and geographical disparities, temporary differences must be considered as a crucial factor. The human values of zones 1 and 2 of the Cathedral of Santiago (Mean and SD = δ^{15}N 11.9 ± 0.4‰, and δ^{13}C − 17.8 ± 0.9‰) are close to those observed in the Cathedral of San Salvador de Oviedo (Mean and SD = δ^{15}N 12.0 ± 1.2‰, and δ^{13}C − 18.6 ± 0.2‰) (MacKinnon et al., 2019). However, we observed a disparity in δ^{15}N when we compared our data with those obtained with the King Pedro I and his court (Mean and SD = δ^{15}N 13.3 ± 1.5‰, and δ^{13}C − 18.6 ± 0.5‰) (Jiménez-Brobeil et al. 2016), or the Cathedral of Santa María de Lugo (Mean and SD = δ^{15}N 13.6 ± 1.3‰, and δ^{13}C − 18.6 ± 0.5‰) (López-Costas et al. 2021). This seems ultimately a reflection of significant socio-economic differences because of the advancement and development of the peninsular Christian kingdoms during the Late Middle Ages (14th and 15th centuries AD). Overall, then, it seems that, by the 9th–12th centuries AD, living in Santiago may have brought certain increased access to meat and marine resources as part of its increasing centrality within a wider religious network. The similarities observed between the individuals in zones 1 and 2 of the Cathedral of Santiago, with those of the Cathedral of San Salvador de Oviedo, corroborate the interpretation that these zones were places reserved for individuals with certain religious, political and/or economic importance for the society of Santiago de Compostela between the 9th and 12th centuries AD.

Conclusions

Our research offers new insights into the beginning and development of Santiago de Compostela following the alleged discovery of the tomb of St James the Great in the 9th century AD and during the following three centuries. Radiocarbon dating has solidified the chronology of the necropolis and its tombs, showing a more complex use of space than was initially interpreted (Guerra Campos 1982). On the basis of measured $^{87}Sr/^{86}Sr$ data, above 50% of the individuals analysed illustrated values potentially indicative of 'non-local' childhoods, particularly for individuals associated with the oldest tomb types (type 'Sarcophagus' and 'Cists'). The combination of strontium and oxygen isotopic data reveals that these 'non-locals' were primarily from a region with environmental conditions similar to those of Santiago of Compostela. Comparison of our data with historical sources suggests that early Santiago may have been populated by individuals from the surrounding rural settlements, the bishop's headquarters of Iria-Flavia (e.g. the bishop Theodomir) and perhaps the wider the Kingdom of Asturias. Wider mobility documented from three individuals may also indicate the possibility of individuals arriving from Al-Andalus—especially priests and bishops who were documented as fleeing Muslim rule during the 9th and 10th centuries AD. Further analysis is required to refine our understanding of scales of mobility within the vicinity of Santiago de Compostela in the future.

The $\delta^{15}N$ and $\delta^{13}C$ results, and the archaeological context, reveal a population with internal socioeconomic divisions that prove the existence of hierarchical society which may have had greater access to certain resources relative to other centres in the same region thanks to its growing religious, political and social status. Our work provides direct information about the origin and development of what was to become one of the biggest mediaeval pilgrimage centres in Europe, allowing us to contrast historical sources with direct insights into diet and mobility from the archaeological remains themselves. Although our human sample size is limited as a result of the destruction of many tombs during previous archaeological excavations, meaning caution should be taken when extrapolating our findings, we believe that our methodological approach holds much promise for future investigations of the emergence of Santiago de Compostela as a European mediaeval religious centre and its impacts on the diets, mobility and cultural behaviours of its inhabitants as part of networks that pilgrims still tread into the 21st century.

Declarations

References

Abuhjeeleh M (2019) Rethinking tourism in Saudi Arabia: royal vision 2030 perspective. African J Hosp Tour Leis 8(5):1–16

Adams S, Grün R, McGahan D, Zhao J-X, Feng Y, Nguyen A, Willmes M, Quaresimin M, Lobsey B, Collard M, Westaway MC (2019) A strontium isoscape of north-east Australia for human provenance and repatriation. Geoarchaeology 34(3):231–251. https://doi.org/10.1002/gea.21728

Adamson MW (2004) Food in medieval times (Greenwood Press).

Agencia Estatal de Meteorología, www.aemet.es.

Alexander MM, Gerrard CM, Gutiérrez A, Millard AR (2015) Diet, society, and economy in late medieval Spain: stable isotope evidence from muslims and christians from Gandía. Valencia Am J Phys Anthropol 156(2):263–273. https://doi.org/10.1002/ajpa.22647

Alertan por los vertidos que sufren en Santiago los ríos Sar y Sarela, September 20th, 2006, https://www.elcorreogallego.es/hemeroteca/alertan-vertidos-sufren-santiago-r-sar-sarela-ECCG82314.

AlQahtani SJ, Hector MP, Liversidge HM (2010) Brief communication: the London atlas of human tooth development and eruption. Am J Phys Anthropol 142(3):481–490. https://doi.org/10.1002/ajpa.21258

Álvarez-Sousa A (2015) Imagen, lealtad y promoción turística Análisis con ecuaciones estructurales. PASOS Rev Tur y Patrim Cult 13(3):629–648. https://doi.org/10.25145/j.pasos.2015.13.044

Ambrose SH, Norr L (1993) Experimental evidence for the relationship of the carbon isotope ratios of whole diet and dietary protein to those of bone collagen and carbonate. In: Lambert JB, Grupe G (eds) Prehistoric human bone. Springer, Berlin, pp 1–37. https://doi.org/10.1007/978-3-662-02894-0_1

Amundson R, Austin AT, Schuur EAG, Yoo K, Matzek V, Kendall C, Uebersax A, Brenner D, Baisden WT (2003) Global patterns of the isotopic composition of soil and plant nitrogen. Global Biogeochem Cycles 17(1):1031. https://doi.org/10.1029/2002GB001903

Andrade Cernadas JM (2009) En el refectorio: la alimentación en el mundo monástico de la Galicia medieval. SEMATA 21:45–64

Araguas-Araguasa LJ, Diaz Teijeiro MF (2005) Isotope composition of precipitation and water vapour in the Iberian Peninsula. In: International Atomic Energy Agency, Isotope Hydrology Section. Isotopic composition of precipitation in the Mediterranean Basin in relation to air circulation patterns and climate. Final report of a coordinated research project 2000–2004, pp 173–190.

Bataille CP, Crowley BE, Wooller MJ, Bowen GJ (2020) Advances in global bioavailable strontium isoscapes. Palaeogeogr Palaeoclimatol Palaeoecol 555:109849. https://doi.org/10.1016/j.palaeo.2020.109849

Bartelink EJ, Chesson LA (2019) Recent applications of isotope analysis to forensic anthropology. Forensic Sci Res 4(1):29–44. https://doi.org/10.1080/20961790.2018.1549527

Bass WH (2005) Human osteology: a laboratory and field manual. Missouri Archaeological Society, Missouri

Bea F, Montero P, Zinger T (2003) The nature, origin, and thermal influence of the granite source layer of Central Iberia. J Geol 111(5):579–595. https://doi.org/10.1086/376767

Beaumont J, Gledhill A, Lee-Thorp J, Montgomery JA (2013) Childhood diet: a closer examination of the evidence from dental tissues using stable isotope analysis of incremental human dentine. Archaeometry 55(2):277–295

Beaumont J, Montgomery J (2015) Oral histories: a simple method of assigning chronological age to isotopic values from human dentine collagen. Ann Hum Biol 42(4):407–414. https://doi.org/10.3109/03014460.2015.1045027

Beaumont J, Montgomery J, Buckberry J, Jay M (2015) Infant mortality and isotopic complexity: new approaches to stress, maternal health, and weaning. Am J Phys Anthropol 157(3):441–457

Blank M, Sjögren K-G, Knipper C, Frei KM, Storå J (2018) Isotope values of the bioavailable strontium in inland southwestern Sweden: a baseline for mobility studies. PLoS ONE 13(10):e0204649. https://doi.org/10.1371/journal.pone.0204649

Bogaard A, Heaton THE, Poulton P, Merbach I (2007) The impact of manuring on nitrogen isotope ratios in cereals: archaeological implications for reconstruction of diet and crop management practices. J Archaeol Sci 34(3):335–343. https://doi.org/10.1016/j.jas.2006.04.009

Britton K (2019) Isotope analysis for mobility and climate studies. In Archaeological science. Cambridge University Press, Cambridge, pp 99–124. https://doi.org/10.1017/9781139013826.005

Britton K, Le Corre M, Willmes M, Moffat I, Grün R, Mannino MA, Woodward S, Jaouen K (2020) Sampling plants and malacofauna in $^{87}Sr/^{86}Sr$ bioavailability studies: Implications for isoscape mapping and reconstructing of past mobility patterns. Front Ecol Evol. https://doi.org/10.3389/fevo.2020.579473

Brock F, Geoghegan V, Thomas B, Jurkschat K, Higham TFG (2013) Analysis of bone "collagen" extraction products for radiocarbon dating. Radiocarbon 55(2):445–463. https://doi.org/10.1017/s0033822200057581

Bronk Ramsey C (2017) Methods for summarizing radiocarbon datasets. Radiocarbon 59(6):1809–1833. https://doi.org/10.1017/RDC.2017.108

Brooks S, Suchey JM (1990) Skeletal age determination based on the os pubis: a comparison of the Acsádi-Nemeskéri and Suchey-Brooks methods. Hum Evol 5:227–238. https://doi.org/10.1007/BF02437238

Brothwell DR (1981) Digging up bones. The excavation, treatment and study of human skeletal remains. Cornell University Press, New York.

Buikstra JE, Ubelaker DH (1994) Measurement of adult remains. In: Haas J, Buikstra JE, Ubelaker DH, Aftandilian D (eds) Standards for data collection from human skeletal remains: proceedings of a seminar at the Field Museum of Natural History. Arkansas Archeological Survey.

Carro Otero J, Varela Ogando ML (1982) Reflexiones sobre la tumba y esqueleto atribuidos al Obispo Teodomiro de Iria. Compostellanum 27(1–3):33–56

Casado J, Brigden K, Santillo D, Johnston P (2019) Screening of pesticides and veterinary drugs in small streams in the European Union by liquid chromatography high resolution mass spectrometry. Sci Total Environ 670:1204–1225. https://doi.org/10.1016/j.scitotenv.2019.03.207

Casey MM, Post DM (2011) The problem of isotopic baseline: reconstructing the diet and trophic position of fossil animals. Earth Sci Rev 106(1):131–148. https://doi.org/10.1016/j.earscirev.2011.02.001

Cenname A (2016) El romance andalusí y los trasvases demográficos y culturales en la Iberia medieval. Normas 6:2174–7245. https://doi.org/10.7203/normas.6.8215

Chamoso Lamas M (1957) Excavaciones arqueológicas en la Catedral de Santiago (Tercera Fase). Compostellanum 2(4):575–619

Chenery CA, Pashley V, Lamb AL, Sloane HJ, Evans JA (2012) The oxygen isotope relationship between the phosphate and structural carbonate fractions of human bioapatite. Rapid Commun Mass Spectrom 26(3):309–319. https://doi.org/10.1002/rcm.5331

Collins-Kreiner N (2010) Researching pilgrimage: continuity and transformations. Ann Tour Res 37(2):440–456. https://doi.org/10.1016/j.annals.2009.10.016

Collins-Kreiner N, Kliot N (2000) Pilgrimage tourism in the Holy Land: the behavioural characteristics of Christian pilgrims. GeoJournal 50:55–67. https://doi.org/10.1023/A:1007154929681

Daux V, Lécuyer C, Héran M-A, Amiot R, Simon L, Fourel F, Martineau F, Lynnerup N, Reychler H, Escarguel G (2008) Oxygen isotope fractionation between human phosphate and water revisited. J Hum Evol 55(6):1138–1147. https://doi.org/10.1016/j.jhevol.2008.06.006

DeNiro MJ (1985) Postmortem preservation and alteration of in vivo bone collagen isotope ratios in relation to palaeodietary reconstruction. Nature 317:806–809. https://doi.org/10.1038/317806a0

DeNiro MJ, Epstein S (1981) Influence of diet on the distribution of nitrogen isotopes in animals. Geochim Cosmochim Acta 45(3):341–351. https://doi.org/10.1016/0016-7037(81)90244-1

Díaz-del-Río P, Waterman AJ, Thomas JT, Peate DW, Tykot RH, Martínez-Navarrete MI, Vicent JM (2017) Diet and mobility patterns in the Late Prehistory of central Iberia (4000–1400 cal bc): the evidence of radiogenic (^{87}Sr/^{86}Sr) and stable (δ^{18}O, δ^{13}C) isotope ratios. Archaeol Anthropol Sci 9(7):1439–1452. https://doi.org/10.1007/s12520-017-0480-y

Díaz-Zorita Bonilla M, Beck J, Bocherens H, Díaz-del-Río P (2018) Isotopic evidence for mobility at large-scale human aggregations in Copper Age Iberia: the mega-site of Marroquíes. Antiquity 92(364):991–1007. https://doi.org/10.15184/aqy.2018.33

Drucker DG, Bridault A, Hobson KA, Szuma E, Bocherens H (2008) Can carbon-13 in large herbivores reflect the canopy effect in temperate and boreal ecosystems? Evidence from modern and ancient ungulates. Palaeogeogr Palaeoclimatol Palaeoecol 266(1–2):69–82. https://doi.org/10.1016/j.palaeo.2008.03.020

Dufour E, Bocherens H, Mariotti A (1999) Palaeodietary implications of isotopic variability in Eurasian lacustrine fish. J Archaeol Sci 26(6):617–627. https://doi.org/10.1006/jasc.1998.0379

Evans J, Stoodley N, Chenery C (2006) A strontium and oxygen isotope assessment of a possible fourth century immigrant population in a Hampshire cemetery, southern England. J Archaeol Sci 33(2):265–272. https://doi.org/10.1016/j.jas.2005.07.011

Evans JA, Chenery CA, Montgomery J (2012) A summary of strontium and oxygen isotope variation in archaeological human tooth enamel excavated from Britain. J Anal at Spectrom 27(5):754–764. https://doi.org/10.1039/c2ja10362a

Evans JA, Montgomery J, Wildman G, Boulton N (2010) Spatial variations in biosphere ^{87}Sr/^{86}Sr in Britain. J Geol Soc 167(1):1–4. https://doi.org/10.1144/0016-76492009-090

Fahy GE, Deter C, Pitfield R, Miszkiewicz JJ, Mahoney P (2017) Bone deep: variation in stable isotope ratios and histomorphometric measurements of bone remodelling within adult humans. J Archaeol Sci 87:10–16. https://doi.org/10.1016/j.jas.2017.09.009

Fernandes R, Nadeau MJ, Grootes PM (2012) Macronutrient-based model for dietary carbon routing in bone collagen and bioapatite. Archaeol Anthropol Sci 4(4):291–301. https://doi.org/10.1007/s12520-012-0102-7

Fernandes R, Rinne C, Nadeau M-J, Grootes P (2016) Towards the use of radiocarbon as a dietary proxy: establishing a first wide-ranging radiocarbon reservoir effects baseline for Germany. Environ Archaeol 21:285–294. https://doi.org/10.1179/1749631414Y.0000000034

Freeman C (2011) Holy bones, holy dust: how relics shaped the history of medieval Europe. Yale University Press, New Haven, CT

Froehle AW, Kellner CM, Schoeninger MJ (2012) Multivariate carbon and nitrogen stable isotope model for the reconstruction of prehistoric human diet. Am J Phys Anthropol 147(3):352–369. https://doi.org/10.1002/ajpa.21651

Gerrard C, Gutiérrez-González JA (2018) Looking south: Spain and Portugal in the Middle Ages. In: Gutiérrez A (ed) Gerrard C, A. The Oxford Handbook of Later Medieval Archaeology in Britain. Oxford University Press, Oxford, pp 964–981

González PA (2018) The Camino is alive: minor logics and commodification in the Camino de Santiago. Anthropol Q 91(3):969–1000. https://doi.org/10.1353/anq.2018.0046

Grau-Sologestoa I (2017) Socio-economic status and religious identity in medieval Iberia: the zooarchaeological evidence. Environ Archaeol 22(2):189–199

Graustein WC (1989) 87Sr/86Sr ratios measure the sources and flow of strontium in terrestrial ecosystems. In: Rundel PW, Ehleringer JR, Nagy KA (eds) Stable isotopes in ecological research. Springer, Berlin, pp 491–512. https://doi.org/10.1007/978-1-4612-3498-2_28.

Grimstead DN, Nugent S, Whipple J (2017) Why a standardization of strontium isotope baseline environmental data is needed and recommendations for methodology. Adv Archaeol Pract 5(2):1–12. https://doi.org/10.1017/aap.2017.6

Grumett D, Muers R (2010) Theology on the menu: asceticism, meat and Christian diet. Routledge

Guede I, Ortega LA, Cruz Zuluaga M, Alonso-Olazabal A, Murelaga X, Solaun JL, Sanchez I, Azkarate A (2018) Isotopic evidence for the reconstruction of diet and mobility during village formation in the Early Middle Ages: Las Gobas (Burgos, northern Spain). Archaeol Anthropol Sci 10(8):2047–2058. https://doi.org/10.1007/s12520-017-0510-9

Guerra Campos J (1982) Exploraciones arqueológicas en torno al sepulcro del Apóstol Santiago. Cabildo de la Catedral de Santiago, Santiago de Compostela.

Gregoricka LA, Sheridan SG, Schirtzinger M (2017) Reconstructing life histories using multi-tissue isotope analysis of commingled remains from St Stephen's Monastery in Jerusalem: limitations and potential. Archaeometry 59(1):148–163. https://doi.org/10.1111/arcm.12227

Hamilton J, Thomas R (2012) Pannage, pulses and pigs: isotopic and zooarchaeological evidence for changing pig management practices in later medieval England. Mediev Archaeol 56(1):234–259

Hamilton M, Nelson SV, Fernandez DP, Hunt KD (2019) Detecting riparian habitat preferences in "savanna" chimpanzees and associated Fauna with strontium isotope ratios: implications for reconstructing habitat use by the chimpanzee-human last common ancestor. Am J Phys Anthropol 170(4):551–564. https://doi.org/10.1002/ajpa.23932

Hammer Ø, Harper DAT, Ryan PD (2001) PAST: paleontological statistics software package for education and data analysis. Palaeontol Electron 4(1):1–9

Hartman G, Richards M (2014) Mapping and defining sources of variability in bioavailable strontium isotope ratios in the Eastern Mediterranean. Geochim Cosmochim Acta 126:250–264. https://doi.org/10.1016/j.gca.2013.11.015

Hedges REM, Reynard LM (2007) Nitrogen isotopes and the trophic level of humans in archaeology. J Archaeol Sci 34(8):1240–1251. https://doi.org/10.1016/j.jas.2006.10.015

Higham T, Ramsey CB, Karavanić I, Smith FH, Trinkaus E (2006) Revised direct radiocarbon dating of the Vindija G1 Upper Paleolithic Neandertals. Proc Natl Acad Sci USA 103(3):553–557. https://doi.org/10.1073/pnas.0510005103

Hill PA (1998) Bone remodelling. Br J Orthod 25(2):101–107. https://doi.org/10.1093/ortho/25.2.101

Holt E, Evans JA, Madgwick R (2021) Strontium (^{87}Sr/^{86}Sr) mapping: a critical review of methods and approaches. Earth Sci Rev 216:103593. https://doi.org/10.1016/j.earscirev.2021.103593

Hoogewerff JA, Reimann C, Ueckermann H, Frei R, Frei KM, van Aswegen T, Stirling C, Reid M, Clayton A, Ladenberger A (2019) Bioavailable ^{87}Sr/^{86}Sr in European soils: a baseline for provenancing studies. Sci Total Environ 672:1033–1044. https://doi.org/10.1016/j.scitotenv.2019.03.387

Howland MR, Corr LT, Young SMM, Jones V, Jim S, van der Merwe NJ, Mitchell AD, Evershed RP (2003) Expression of the dietary isotope signal in the compound-specific $\delta13$C values of pig bone lipids and amino acids. Int J Osteoarchaeol 13(1–2):54–65. https://doi.org/10.1002/oa.658

Jacob E, Querci D, Caparros M, Barroso Ruiz C, Higham T (2018) Devièse T (2018) Nitrogen content variation in archaeological bone and its implications for stable isotope analysis and radiocarbon dating. J Archaeol Sci 93:68–73

James HF, Adams S, Willmes M, Mathison K, Ulrichsen A, Wood R, Valera AC, Frieman CJ, Grün R (2022) A large-scale environmental strontium isotope baseline map of Portugal for archaeological and paleoecological provenance studies. J Archaeol Sci 142:105595. https://doi.org/10.1016/J.JAS.2022.105595

Jim S, Ambrose SH, Evershed RP (2004) Stable carbon isotopic evidence for differences in the dietary origin of bone cholesterol, collagen and apatite: implications for their use in palaeodietary reconstruction. Geochim Cosmochim Acta 68(1):61–72. https://doi.org/10.1016/S0016-7037(03)00216-3

Jiménez-Brobeil SA, Laffranchi Z, Maroto RM, López Sánchez FA, Delgado Huertas A (2016) How royals feasted in the court of Pedro I of Castile: a contribution of stable isotope study to medieval history. J Archaeol Sci Rep 10:424–430. https://doi.org/10.1016/j.jasrep.2016.11.010

Kaal J, López-Costas O, Martínez Cortizas A (2016) Diagenetic effects on pyrolysis fingerprints of extracted collagen in archaeological human bones from NW Spain, as determined by pyrolysis-GC-MS. J Archaeol Sci 65:1–10. https://doi.org/10.1016/j.jas.2015.11.001

Kim B, Kim SS, King B (2016) The sacred and the profane: identifying pilgrim traveler value orientations using means-end theory. Tour Manag 56:142–155. https://doi.org/10.1016/j.tourman.2016.04.003

Klales AR, Ousley SD, Vollner JM (2012) A revised method of sexing the human innominate using Phenice's nonmetric traits and statistical methods. Am J Phys Anthropol 149(1):104–114

Larsson M, Magnell O, Styring A, Lagerås P, Evans J (2020) Movement of agricultural products in the Scandinavian Iron Age during the first millennium AD: ^{87}Sr/^{86}Sr values of archaeological crops and animals in southern Sweden. Sci Technol Archaeol Res 6(1):96–112. https://doi.org/10.1080/20548923.2020.1840121

Lécolle P (1985) The oxygen isotope composition of landsnail shells as a climatic indicator: applications to hydrogeology and paleoclimatology. Chem Geol Isot Geosci Sect 58(1–2):157–181. https://doi.org/10.1016/0168-9622(85)90036-3

Levinson AA, Luz B, Kolodny Y (1987) Variations in oxygen isotopic compositions of human teeth and urinary stones. Appl Geochemistry 2(4):367–371. https://doi.org/10.1016/0883-2927(87)90021-7

Lightfoot E, O'Connell TC (2016) On the use of biomineral oxygen isotope data to identify human migrants in the archaeological record: intra-sample variation, statistical methods and geographical considerations. PLoS ONE 11:e0153850. https://doi.org/10.1371/journal.pone.0153850

Longinelli A (1984) Oxygen isotopes in mammal bone phosphate: a new tool for paleohydrological and paleoclimatological research? Geochim Cosmochim Acta 48(2):385–390. https://doi.org/10.1016/0016-7037(84)90259-X

López Alsina F (1990) De la magna congregatio al cabildo e Santiago: reformas del clero catedralicio (830–1110). Actas Congreso Internacional IX Centenário da Dedicaçao da Sé de Braga, vol 1. Universidade de Braga, Braga, pp 735–762

López Alsina F (2015) La ciudad de Santiago de Compostela en la Alta Edad Media. Consorcio de Santiago, Santiago de Compostela.

López-Costas O, Müldner G (2016) Fringes of the empire: diet and cultural change at the Roman to post-Roman transition in NW Iberia. Am J Phys Anthropol 161(1):141–154. https://doi.org/10.1002/ajpa.23016

López-Costas O, Müldner G (2018) Boom and bust at a medieval fishing port: dietary preferences of fishers and artisan families from Pontevedra (Galicia, NW Spain) during the Late Medieval and Early Modern Period. Archaeol Anthropol Sci 11(8):3717–3731. https://doi.org/10.1007/s12520-018-0733-4

López-Costas O, Müldner G, Lidén K (2021) Biological histories of an elite: skeletons from the Royal Chapel of Lugo Cathedral (NW Spain). Int J Osteoarchaeol 31:941–956. https://doi.org/10.1002/oa.3011

López-Costas O, Teira Brión A (2014) Condiciones de vida reconstruidas mediante el estudio de los restos humanos hallados en la fortaleza Bajomedieval de A Rocha Forte, Santiago de Compostela.

Gall Rev Arqueol e antigüidade 33:257–280. https://doi.org/10.15304/gall.33.2309

López Quiroga J (2018) Redimensionando el estudio del mundo funerario tardo-antiguo Pervivencia y transformación en los ritos y prácticas mortuorias en la Gallaecia de época sueva. In In: López Quiroga J (ed) Tempore Sueborum. El tiempo de los Suevos en la Gallaecia (411–585). El primer reino medieval de Occidente. Servicio de Publicaciones de la Diputación Provincial de Ourense, Ourense, pp 421–438.

Lovejoy CO, Meindl RS, Pryzbeck TR, Mensforth RP (1985) Chronological metamorphosis of the auricular surface of the ilium: a new method for the determination of adult skeletal age at death. Am J Phys Anthropol 68:15–28. https://doi.org/10.1002/ajpa.1330680103

Lubritto C, García-Collado MI, Ricci P, Altieri S, Sirignano C, Quirós Castillo JA (2017) New dietary evidence on medieval rural communities of the Basque Country (Spain) and its surroundings from carbon and nitrogen stable isotope analyses: social insights, diachronic changes and geographic comparison. Int J Osteoarchaeol 27(6):984–1002. https://doi.org/10.1002/oa.2610

MacKinnon AT, Passalacqua NV, Bartelink EJ (2019) Exploring diet and status in the medieval and modern periods of Asturias, Spain, using stable isotopes from bone collagen. Archaeol Anthropol Sci 11(3):3837–3855

Makarewicz CA, Sealy J (2015) Dietary reconstruction, mobility, and the analysis of ancient skeletal tissues: expanding the prospects of stable isotope research in archaeology. J Archaeol Sci 56:146–158. https://doi.org/10.1016/j.jas.2015.02.035

Männel TT, Auerswald K, Schnyder H (2007) Altitudinal gradients of grassland carbon and nitrogen isotope composition are recorded in the hair of grazers. Glob Ecol Biogeogr 16(5):583–592. https://doi.org/10.1111/j.1466-8238.2007.00322.x

Martínez Díez G (2011) La migración mozárabe al Reino de León, siglos IX y X. Antigüedad y Cristianismo 28:99–117

Martínez Catalán JR, Klein E, Pablo Maciá JG, González Lodeiro F (1984) El complejo de Órdenes: subdivisión, descripción y discusión sobre su origen. Cadernos do Laboratorio Xeolóxico de Laxe 7:139–210

Martínez García, L. (2004) El Camino de Santiago: Una visión histórica desde Burgos (Caja Círculo).

Maurer AF, Galer SJG, Knipper C, Beierlein L, Nunn EV, Peters D, Tütken T, Alt KW, Schöne BR (2012) Bioavailable 87Sr/ 86Sr in different environmental samples - effects of anthropogenic contamination and implications for isoscapes in past migration studies. Sci Total Environ. https://doi.org/10.1016/j.scitotenv.2012.06.046

Mays S (2010) The archaeology of human bones, 2nd edn. Routledge, London

Meindl RS, Lovejoy CO (1985) Ectocranial suture closure: a revised method for the determination of skeletal age at death based on the lateral-anterior sutures. Am J Phys Anthropol 68(1):57–66. https://doi.org/10.1002/ajpa.1330680106

Millán Vásquez de la Torre MG, Morales Fernández E, Pérez Naranjo LM (2010) Turismo religioso: Estudio del Camino de Santiago. Gestión Turística 13:9–37. https://doi.org/10.4206/gest.tur.2010.n13-01

Miller EK, Blum JD, Friedland AJ (1993) Determination of soil exchangeable-cation loss and weathering rates using Sr isotopes. Nature 362:438–441. https://doi.org/10.1038/362438a0

Miranda García F (2002) La «crisis» del siglo XVI. In: Álvarez Palenzuela VA (ed) Historia universal de la Edad Media. Ariel, Madrid, pp 647–662

Molénat J-P (2019) Toledo, siglos XII-XV La coexistencia de cristianos (latinos y mozárabes), musulmanes y judíos. Una síntesis. Al Qantara 40(2):385–405. https://doi.org/10.3989/alqantara.2019.012

Montgomery J (2010) Passports from the past: investigating human dispersals using strontium isotope analysis of tooth enamel. Ann Hum Biol 37(3):325–346. https://doi.org/10.3109/03014461003649297

Muldner G, Montgomery J, Cook G, Ellam R, Gledhill A, Lowe C (2009) Isotopes and individuals: diet and mobility among the medieval bishops of Whithorn. Antiquity 83(322):1119–1133. https://doi.org/10.1017/S0003598X00099403

Mundee M (2010) An isotopic approach to diet in medieval Spain. In: Baker S, Gray A, Lakin K, Madgwick R, Poole K, Sandias M (Eds) Food and drink in archaeology 2. University of Nottingham Postgraduate Conference, Nottingham, pp 64–72.

Pallares Méndez MC, Portela Silva E (1975) Aproximación al estudio de las explotaciones agrarias de Galicia durante los siglos IX al XII. Actas de las I Jornadas de Metodología Aplicada de las Ciencias Históricas, vol 2. Universidade de Santiago de Compostela, Santiago de Compostela, pp 95–113

Passini J (1993) El espacio urbano a lo largo del Camino de Santiago. In: El Camino de Santiago y la articulación del espacio Hispánico. XX Semana de Estudios Medievales, Estella. Gobierno de Navarra, Pamplona, pp 247–269.

Pedreira Barros I (1972) Los Esqueletos 1, b, f y g de la necrópolis germánica subyacente a la Catedral de Santiago. Doctoral Thesis (Universidad de Santiago de Compostela).

Peña-Chocarro L, Pérez-Jordà G, Alonso N, Antolín F, Teira-Brión A, Tereso JP, Montes Moya EM, López Reyes D (2019) Roman and medieval crops in the Iberian Peninsula: a first overview of seeds and fruits from archaeological sites. Quat Int 499:49–66. https://doi.org/10.1016/j.quaint.2017.09.037

Pérez de Tudela y Velasco MI (1998) Guerra, violencia y terror. La destrucción de Santiago de Compostela por Almanzor hace mil años. La España Medieval 21:9–28

Pérez Ramallo P (2015) Pilgrimage to Santiago de Compostela: investigating society and the geographical mobility of medieval individuals. Master Dissertation. Universirty of Bradford, Bradford, the UK.

Pérez Ramallo, P. (2021) Pilgrimage to Santiago de Compostela: osteological and biomolecular análisis of medieval individuals. Doctoral thesis. University of the Basque Country, Donostia-San Sebastián, Spain.

Pérez-Ramallo P, Lorenzo-Lizalde JI, Staniewska A, Lopez B, Alexander M, Marzo S, Lucas M, Ilgner J, Chivall D, Grandal-dAnglade A, Roberts P (2022) Stable isotope analysis and differences in diet and social status in northern Medieval Christian Spain (9th–13th centuries CE). J Archaeol Sci Rep 41:103325. https://doi.org/10.1016/J.JASREP.2021.103325

Pérez Samper MA (2019) Comer y beber. Una historia de la alimentación en España. Cátedra, Barcelona.

Pin C, Briot D, Bassin C, Poitrasson F (1994) Concomitant separation of strontium and samarium-neodymium for isotopic analysis in silicate samples, based on specific extraction chromatography. Anal Chim Acta 298(2):209–217. https://doi.org/10.1016/0003-2670(94)00274-6

Ramírez Pascual T (2004) Milagros de peregrinos a Santiago: edición, traducción y estudio de la narración de varios "milagros de peregrinos" conservada en un Códice del Archivo de la Catedral de Santo Domingo de la Calzada. Berceo 146:109–136

Reimer PJ, Austin WEN, Bard E, Bayliss A, Blackwell PG, Bronk Ramsey C, Butzin M, Cheng H, Edwards RL, Friedrichet M et al (2020) The IntCal20 northern hemisphere radiocarbon age calibration curve (0–55 cal kBP). Radiocarbon 62(4):725–757. https://doi.org/10.1017/RDC.2020.41

Richards MP, Hedges REM (1999) Stable isotope evidence for similarities in the types of marine foods used by late Mesolithic humans at sites along the Atlantic coast of Europe. J Archaeol Sci 26(6):717–722. https://doi.org/10.1006/jasc.1998.0387

Rosener W (1992) Peasants in the Middle Ages. University of Illinois Press

Salazar-García DC, Richards MP, Nehlich O, Henry AG (2014) Dental calculus is not equivalent to bone collagen for isotope analysis: a comparison between carbon and nitrogen stable isotope analysis of bulk dental calculus, bone and dentine collagen from same individuals from the medieval site of El Raval (Alicante, Spain). J Archaeol Sci 47:70–77. https://doi.org/10.1016/j.jas.2014.03.026

Scaffidi BK, Tung TA, Gordon G, Alaica AK, González La Rosa LM, Marsteller SJ, Dahlstedt A, Schach E, Knudson KJ (2020) Drinking locally: a water $^{87}Sr/^{86}Sr$ isoscape for geolocation of archeological samples in the Peruvian Andes. Front Ecol Evol. https://doi.org/10.3389/fevo.2020.00281

Schoeninger MJ, DeNiro MJ (1984) Nitrogen and carbon isotopic composition of bone collagen from marine and terrestrial animals. Geochim Cosmochim Acta 48(4):625–639. https://doi.org/10.1016/0016-7037(84)90091-7

Sealy JC, van der Merwe NJ, Thorp JAL, Lanham JL (1987) Nitrogen isotopic ecology in southern Africa: implications for environmental and dietary tracing. Geochim Cosmochim Acta 51(10):2707–2717. https://doi.org/10.1016/0016-7037(87)90151-7

Serrano Pinto M, Casquet C, Ibarrola E, Corretge LG, Portugal Ferreira M (1988) Sintese geocronológica dos granitoides do Maciço Hespérico. In: Bea F., Carnicero, A, Gonzalo JC, Lopez Plaza M, Rodríguez Alonso MD (eds) Geología de los granitoides y rocas asociadas del Macizo Hespérico. Rueda, pp 69–86.

Smith BN, Epstein S (1971) Two categories of 13C/12C ratios for higher plants. Plant Physiol 47(3):380–384

Suárez J, Ardá I, González J, Puertas J, García R, Álvarez M, Vieito S (2009) Modelización de la calidad del agua en ríos fuertemente contaminados por aguas residuales urbanas: experiencias en el río Sar (Galicia). Jornadas de Ingeniería del Agua, 27 y 28 de Octubre, Madrid, España.

Suárez Otero J (2015) Locus Iacobi: orígenes de un santuario de peregrinación. Doctoral Thesis, Universidade de Santiago de Compostela, Spain.

Sulai Capponi A (2006) El culto de Santiago: de Matamoros a Mataindios; de patrón de los conquistadores a santo de los indios. XXVIII Convegno Internazionale di Americanistica, 979–985.

Tieszen LL, Fagre T (1993) Effect of diet quality and composition on the isotopic composition of respiratory CO2, bone collagen, bioapatite, and soft tissues. In: Lambert JB, Grupe G (eds) Prehistoric human bone. Springer, Berlin, pp 121–155. https://doi.org/10.1007/978-3-662-02894-0_5

Toso A, Gaspar S, Banha da Silva R, Garcia SJ, Alexander M (2019) High status diet and health in medieval Lisbon: a combined isotopic and osteological analysis of the Islamic population from São Jorge Castle, Portugal. Archaeol Anthropol Sci 11:3699–3716. https://doi.org/10.1007/s12520-019-00822-7

van Klinken GJ (1999) Bone collagen quality indicators for palaeodietary and radiocarbon measurements. J Archaeol Sci 26(6):687–695. https://doi.org/10.1006/jasc.1998.0385

Vijayanand S (2012) Socio-economic impacts in pilgrimage tourism. Zenith: Int J Multidiscip Res 2(1): 329–343.

Voerkelius S, Lorenz GD, Rummel S, Quétel CR, Heiss G, Baxter M, Brach-Papa C, Deters-Itzelsberger P, Hoelzl S, Hoogewerff J, Ponzevera E, Van Bocxstaele M, Ueckermann H (2010) Strontium isotopic signatures of natural mineral waters, the reference to a simple geological map and its potential for authentication of food. Food Chem 118(4):933–940. https://doi.org/10.1016/j.foodchem.2009.04.125

Walker PL (2008) Sexing skulls using discriminant function analysis of visually assessed traits. Am J Phys Anthropol 136(1):39–50. https://doi.org/10.1002/ajpa.20776

Waterman AJ, Peate DW, Silva AM, Thomas JT (2014) In search of homelands: using strontium isotopes to identify biological markers of mobility in late prehistoric Portugal. J Archaeol Sci 28:119–127. https://doi.org/10.1016/j.jas.2013.11.004

Webb EC, White CE, Longstaffe FJ (2014) Investigating inherent differences in isotopic composition between human bone and enamel bioapatite: Implications for reconstructing residential histories. J Archaeol Sci 50:97–107. https://doi.org/10.1016/j.jas.2014.07.001

Wright LE, Schwarcz HP (1999) Correspondence between stable carbon, oxygen and nitrogen isotopes in human tooth enamel and dentine: Infant diets at Kaminaljuyu. J Archaeol Sci. https://doi.org/10.1006/jasc.1998.0351

http://www.waterisotopes.org. Gridded maps of the isotopic composition of meteoric waters (Internet).

Yoder C (2012) Let them eat cake? Status-based differences in diet in medieval Denmark. J Archaeol Sci 39(4):1183–1193. https://doi.org/10.1016/j.jas.2011.12.029

Authors and Affiliations

Patxi Pérez-Ramallo[1,2,3] · Aurora Grandal-d´Anglade[4] · Elia Organista[5,6] · Elena Santos[7] · David Chivall[8] · Ricardo Rodríguez-Varela[9,10] · Anders Götherström[9,10] · Francisco Etxeberria[3] · Jana Ilgner[1,2] · Ricardo Fernandes[2,11,12] · Juan Luis Arsuaga[13] · Petrus Le Roux[14] · Tom Higham[15] · Julia Beaumont[16] · Hannah Koon[16] · Patrick Roberts[1,2,17]

1   isoTROPIC Research Group, Max Planck Institute for Geoanthropology, Kahlaische Str. 10, 07745 Jena, Germany

2   Department of Archaeology, Max Planck Institute for Geoanthropology, Kahlaische Str. 10, 07745 Jena, Germany

3   Departamento de Especialidades Médico-Quirúrgicas, Facultad de Medicina y Enfermería, University of the Basque Country (EHU), Donostia-San Sebastián, Spain

4   Instituto Universitario de Xeoloxía, Universidade da Coruña (UDC), ESCI 15071, A Coruña, Spain

5   Osteoarcheological Research Laboratory, Department of Archaeology and Classical Studies, Stockholm University, 106 91 Stockholm, Sweden

6   Institute of Evolution in Africa (IDEA), University of Alcalá de Henares, 28010 Madrid, Spain

7   University of Burgos (UBu), Burgos, Spain

8   Oxford Radiocarbon Accelerator Unit, Research Laboratory for Archaeology and the History of Art, University of Oxford, Oxford OX13QY, UK

9   Centre for Palaeogenetics, 106 91 Stockholm, Sweden

10 Department of Archaeology and Classical Studies, Stockholm University, 10691 Stockholm, Sweden

11 Climate Change and History Research Initiative, Princeton University, Princeton, NJ, USA

12 Faculty of Arts, Masaryk University, Brno, Czech Republic

13 Universidad Complutense de Madrid, Centro Mixto UCM-ISCIII, Madrid, Spain

14 Department of Geological Sciences, University of Cape Town, Cape Town, South Africa

15 Research Network Human Evolution and Archaeological Sciences (HEAS), Department of Evolutionary Anthropology, University of Vienna, Vienna, Austria

16 School of Archaeological and Forensic Sciences, Faculty of Life Sciences, University of Bradford, Bradford, UK

17 School of Social Sciences, University of Queensland, St Lucia Brisbane, QLD 4072, Australia